A STUDY OF VETIVER-POLYPROPYLENE COMPOSITES

Miss Wandee Thuamthong

A Thesis Submitted in Partial Fulfillment of the Requirements for the

Degree of Master of Engineering in Polymer Engineering

Suranaree University of Technology

Academic Year 2004

ISBN 974-533-360-3

การศึกษาวัสดุเชิงประกอบระหว่างหญ้าแฝกและพอลิโพรพิลีน

นางสาววันดี ท้วมทอง

วิทยานิพนธ์นี้เป็นส่วนหนึ่งของการศึกษาตามหลักสูตรปริญญาวิศวกรรมศาสตรมหาบัณฑิต

สาขาวิชาวิศวกรรมพอลิเมอร์

มหาวิทยาลัยเทคโนโลยีสุรนารี

ปีการศึกษา 2547

ISBN 974-533-360-3

A STUDY OF VETIVER-POLYPROPYLENE COMPOSITES

Suranaree University of Technology has approved this thesis submitted in partial fulfillment of the requirements for a Master's Degree.

Thesis Examining Committee

(Asst. Prof. Dr.Utai Meekum)

Chairperson

(Asst. Prof. Dr.Yupaporn Ruksakulpiwat)

Member (Thesis Advisor)

(Dr.Wimonlak Sutapun)

Member

(Dr.Nitinat Suppakarn)

Member

(Asst. Prof. Dr.Visit Vao-soongnern)

Member

(Assoc. Prof. Dr.Sarawut Sujitjorn)

Vice Rector for Academic Affairs

(Assoc. Prof. Dr.Vorapot Khompis)

Dean of Institute of Engineering

วันดี ท้วมทอง การศึกษาวัสดุเชิงประกอบระหว่างหญ้าแฝกและพอลิโพรพิลีน (A STUDY OF VETIVER-POLYPROPYLENE COMPOSITES) อาจารย์ที่ปรึกษา : ผู้ช่วยศาสตราจารย์ ดร.ยุพาพร รักสกุลพิวัฒน์, 90 หน้า. ISBN 974-533-360-3

วิทยานิพนธ์นี้เป็นการศึกษาวัสดุเชิงประกอบระหว่างหญ้าแฝกและพอลิโพรพิลีน หญ้าแฝกที่ใช้ อยู่ในลักษณะของใบหญ้าแฝก และเส้นใยหญ้าแฝก การปรับปรุงสมบัติของหญ้าแฝกโดยกระบวนการทางเคมีทำโดยใช้โซเดียมไฮรดรอกไซค์ และ ไวนิลไตรเมทรอกซีไซเลน วัสดุเชิงประกอบระหว่างหญ้าแฝกและพอลิโพรพิลีนเตรียมที่อัตราส่วนผสม 5 10 20 และ 30 เปอร์เซ็นต์โดยน้ำหนัก วัสดุเชิงประกอบขึ้นรูปเป็นชิ้นทดสอบโดยใช้กระบวนการขึ้นรูปแบบฉีด แล้วทำการตรวจสอบสมบัติทางกายภาพและสมบัติทางความร้อนของหญ้าแฝก รวมทั้งผลของความยาวหญ้าแฝกที่มีต่อสมบัติทางกลของวัสดุเชิงประกอบ และตรวจสอบผลของอัตราส่วนผสม และผลของการปรับปรุงหญ้าแฝกโดยกระบวนการทางเคมีที่มีต่อสมบัติทางความร้อน สมบัติทางวิทยกระแส สมบัติทางกล สมบัติทางสัณฐานวิทยา และการเกิดผลึกโดยการเหนี่ยวนำจากแรงเฉือนของวัสดุเชิงประกอบ

ผลการวิจัยพบว่าวัสดุเชิงประกอบ ที่มีความยาวหญ้าแฝกแตกต่างกันมีสมบัติทางกลที่ไม่แตกต่างกันอย่างมีนัยสำคัญ เมื่อเปรียบเทียบกับพอลิโพรพิลีนที่ไม่ได้ผสมหญ้าแฝกแล้วพบว่า วัสดุเชิงประกอบระหว่างพอลิโพรพิลีนและหญ้าแฝกจะมีค่าความแข็งแรงต่อการดึง ค่ามอดุลัสของยังสูงกว่า แต่มีค่าเปอร์เซ็นต์ความเครียด ณ จุดแตกหัก และความแข็งแรงต่อการกระแทกต่ำกว่า การเพิ่มขึ้นของปริมาณหญ้าแฝกในวัสดุเชิงประกอบส่งผลให้ ความหนืด อุณหภูมิการบิดงอ อุณหภูมิการเกิดผลึก และค่ามอดุลัสของยัง มีค่าเพิ่มขึ้น แต่ในทางตรงกันข้าม อุณหภูมิการเสื่อมสภาพ เปอร์เซ็นต์การเกิดผลึก ความแข็งแรงต่อการดึง เปอร์เซ็นต์ความเครียด ณ จุดแตกหัก และความแข็งแรงต่อการกระแทก มีค่าลดลงเมื่อปริมาณหญ้าแฝกในวัสดุเชิงประกอบเพิ่มขึ้น นอกจากนี้ ภาพถ่ายจากกล้องจุลทรรศน์อิเล็กตรอนแบบส่องกราดของวัสดุเชิงประกอบ ณ บริเวณพื้นที่ผิวที่แตกหัก พบว่ามีการเกาะกลุ่มรวมกันของเส้นใยมากขึ้นเมื่อปริมาณหญ้าแฝกเพิ่มขึ้น อย่างไรก็ตาม เมื่ออัตราส่วนของหญ้าแฝกเพิ่มขึ้นไม่มีผลกระทบต่อ อุณหภูมิการหลอมเหลว และการเกิดผลึกโดยการเหนี่ยวนำจากแรงเฉือน การปรับปรุงโดยกระบวนการทางเคมีทำให้มีการเพิ่มขึ้นของอุณหภูมิการเสื่อมสภาพของหญ้าแฝก และเปอร์เซ็นต์การเกิดผลึกของวัสดุเชิงประกอบ รวมถึงช่วยปรับปรุงสมบัติทางกลของวัสดุเชิงประกอบให้ดีขึ้น อย่างไรก็ดี การปรับปรุงโดยกระบวนการทางเคมีไม่ส่งผลกระทบต่ออุณหภูมิการบิดงอ อุณหภูมิการหลอมเหลว อุณหภูมิการเกิดผลึก และการเกิดผลึกโดยการเหนี่ยวนำจากแรงเฉือนของวัสดุเชิงประกอบ จากภาพถ่ายจากกล้องจุลทรรศน์อิเล็กตรอนแบบส่องกราด พบว่า การใช้โซเดียมไฮรดรอกไซค์ในการปรับปรุงสมบัติของหญ้าแฝกสามารถ

กำจัดสิ่งสกปรกที่ติดอยู่บนเส้นใย และทำให้เส้นใยแยกออกจากกัน ซึ่งช่วยเพิ่มพื้นที่ผิวสัมผัสระหว่างเส้นใยกับพอลิโพรพิลีน

สาขาวิชาวิศวกรรมพอลิเมอร์ ลายมือชื่อนักศึกษา _____

ปีการศึกษา 2547 ลายมือชื่ออาจารย์ที่ปรึกษา _____

ลายมือชื่ออาจารย์ที่ปรึกษาร่วม_____

ลายมือชื่ออาจารย์ที่ปรึกษาร่วม_____

WANDEE THUAMTHONG : A STUDY OF VETIVER-POLYPROPYLENE COMPOSITES. THESIS ADVISOR : ASST. PROF. YUPAPORN RUKSAKULPIWAT, Ph.D. 90 PP. ISBN 974-533-360-3

VETIVER GRASS/ PP-COMPOSITES/ THERMAL/ RHEOLOGICAL/ MECHANICAL/ MORPHOLOGICAL/ SHEAR-INDUCED CRYSTALLIZATION

In this thesis, vetiver-polypropylene (PP) composites were studied. Vetiver grass was employed as vetiver leave and vetiver fiber. The chemical treatment of vetiver grass was performed by using sodium hydroxide (NaOH) and vinyltrimethoxysilane. The vetiver-PP composites were prepared at 5%, 10%, 20%, and 30% vetiver content. The composite specimens were prepared by injection molding. The physical and thermal properties of vetiver grass were investigated. The effect of vetiver length of vetiver-PP composites on mechanical properties was determined. In addition, the effects of vetiver content and chemical treatment on the thermal properties, rheological properties, mechanical properties, morphological properties, and shear-induced crystallization of vetiver-PP composites were examined.

The results showed that the composites at various vetiver lengths showed no significant change in mechanical properties. When compared to PP, vetiver-PP composites exhibited higher tensile strength, Young's modulus but lower elongation at break and impact strength. An increase in vetiver content of the composites led to an increase in viscosity, heat distortion temperature, crystallization temperature, and Young's modulus. On the other hand, the decomposition temperature, % crystallinity, tensile strength, elongation at break, and impact strength decreased with increasing vetiver contents. Moreover, SEM micrographs of fracture surface of the composites

showed more agglomeration of vetiver fiber with increasing vetiver content. However, an increase in vetiver content showed no significant effect on melting temperature and shear-induced crystallization in the composites. Chemical treatment resulted in an increase in the decomposition temperature of vetiver grass and % crystallinity of the composites. In addition, it showed an improvement in the mechanical properties of the composites. However, the chemical treatment showed no effect on heat distortion temperature, melting temperature, crystallization temperature, and shear-induced crystallization of the composites. From SEM micrographs, it showed that NaOH treatment can remove surface impurities and the fibers were well separated. This increased the effective surface area available for contact between fiber and matrix.

School of Polymer Engineering

Academic Year 2004

Student's Signature _____

Advisor's Signature_____

Co-advisor's Signature _____

Co-advisor's Signature _____

ACKNOWLEDGEMENTS

The author wishes to acknowledge the funding support from Suranaree University of Technology (SUT).

The grateful thanks and appreciation are given to the thesis advisor, Asst. Prof. Dr.Yupaporn Ruksakulpiwat, for her consistent supervision, advice and support throughout this project. Special thanks are also extended to Dr.Wimonlak Sutapun and Dr.Nitinat Suppakarn for their valuable suggestion and guidance given as co-thesis advisor.

The author is also grateful to all the faculty and staff members of the School of Polymer Engineering and colleagues for their help and assistance throughout the period of this study.

Finally, I thank my father and mother who support and encourage me throughout the course of this study at the Suranaree University of Technology.

Miss Wandee Thuamthong

TABLES OF CONTENTS

PAGE

TABLES OF CONTENTS (Continued)

PAGE

TABLES OF CONTENTS (Continued)

PAGE

TABLES OF CONTENTS (Continued)

PAGE

LIST OF TABLES

TABLE **PAGE**

LIST OF TABLES (Continued)

TABLE **PAGE**

LIST OF TABLES (Continued)

TABLE **PAGE**

LIST OF FIGURES

FIGURE **PAGE**

LIST OF FIGURES (Continued)

FIGURE **PAGE**

LIST OF FIGURES (Continued)

FIGURE **PAGE**

LIST OF FIGURES (Continued)

FIGURE **PAGE**

SYMBOLS AND ABBREVIATIONS

%	=	Percent
ΔH	=	Heat of fusion
μm	=	Micrometer
°C	=	Degree Celsius
g	=	Gram
cm^3	=	Cubic centimeter
GPa	=	Gigapasca
J	=	Joule
k	=	Kilo
kg	=	Kilogram
kN	=	Kilonewton
kPa	=	Kilopasca
m^2	=	Square meters
mg	=	Milligram
min	=	Minute
mm	=	Millimeter
MPa	=	Megapasca
mW	=	Milliwatt
rpm	=	Revolution per minute
sec	=	Second

SYMBOLS AND ABBREVIATIONS (Continued)

v	=	Volume
w	=	Weight

CHAPTER I

INTRODUCTION

1.1 General introduction

In recent year, natural fibers have been increasingly used as alternative fillers in many areas of polymer composites (Bledzki and Gassan, 1999; Schuh, 1999; Bruijn, 2000). Their advantages over synthetic fibers are low cost, less tool wear during processing, low density, environmental friendly and biodegradability (Saheb and Jog, 1999; Wambua, Iens, and Verpoest, 2003; Mohanty, Misra, and Hinrichsen, 2000). Natural fibers are classified into three types as seed hair, bast fibers, and leaf fibers (Cook,1993). Some examples are cotton (seed hair), ramie, jute, and flax (base fibers), and sisal and abaca (leaf fiber). Of these fibers jute, ramie, flax, and sisal are the most commonly used fibers for polymer composite (Eichhon et al., 2001).

The chemical composition of natural fibers varies which depends on the type of fiber. Generally, the natural fibers contain cellulose, hemicellulose, pectin and lignin. Hemicellulose is responsible for the biodegradation, moisture absorption, and thermal degradation of the fiber. Lignin is thermally stable and it is responsible for the UV degradation. The percent composition of each of these components varies for different fibers (Rowell, 1989). Vetiver grass is one of the interesting candidates. Vetiver grass is a tropical plant which can well adapt to different environment conditions. In Thailand, this grass can be found growing in a wide range of areas. The dominant vetiver grass species grown in Thailand is commonly referred to with its

scientific name as Vetiveria zizanioides. It appears with dense clumps and is fast growing through tillering. The clump's diameter is about 30 cm with a height of 50-150 cm. The narrow, erect and rather stiff leaf is about 75 cm long and 8 mm wide. According to His Majesty the King of Thailand's Royal Initiative, the main purpose of vetiver grass cultivation is to conserve soil and water, particularly for the steep slope areas. In spite of the effort, some farmers are still reluctant to accept its valuable attributes because cultivation of vetiver in agricultural areas in order to conserve soil and water does not produce tangible benefits in terms of revenue. Actually, vetiver leaves and roots can be used for other purposes especially its leaves, which usually have to be cut to keep the vetiver rows in order (Nakorn, Chinapan, and Tepnaraprapai, 1999). This becomes an inspiration of this work to make use of the vetiver grass as filler in polymer composite which can help the farmer gain some extra income.

PP is one of the most used polymers for short fiber reinforced composite due to many advantages. First, it is easy to process and one of the cheapest polymers on the market which is of eminent importance in the 'cost-performance' sector. Second, it has a low processing temperature, which is essential because of the relatively low thermal stability of natural fibers (200-250°C). Finally, it has the perfect ability to protect the hydrophilic nature of the natural fiber because of its strong hydrophobic and non-polar characteristic. However, a disadvantage of this non-polar characteristic for composite applications is its limited wettability as well as poor interfacial bonding with reinforcing fibers. This disadvantage can, however, be overcome by chemical treatment of fibers, which has proven to be very effective in enhancing fiber/matrix adhesion in composite systems based on polyolefins.

1.2 Research objectives

The main objectives of this study are as follow:

(i) To study the effect of vetiver length on mechanical properties of vetiver-PP composites.

(ii) To study the effect of vetiver content and chemical treatment on the thermal properties, rheological properties, mechanical properties, morphological properties, and shear-induced crystallization of vetiver-PP composites.

1.3 Scope and limitation of the study

In this research, vetiver-PP composites were studied. Vetiver grass was employed as vetiver leave and vetiver fiber. The chemical treatment of vetiver grass was done by using NaOH and vinyltrimethoxysilane. The vetiver-PP composites were prepared by mixing PP and vetiver grass at various vetiver contents in the internal mixer. The composite specimens were prepared by injection molding. The physical and thermal properties of vetiver grass were investigated. The effect of vetiver length and mixing procedure of vetiver-PP composites on mechanical properties were determined. In addition, the effect of vetiver content and chemical treatment on the thermal properties, rheological properties, mechanical properties, morphological properties, and shear-induced crystallization of vetiver-PP composites were examined.

CHAPTER II

LITERATURE REVIEW

2.1 The study of natural fibers reinforced composites on mechanical properties

During the past decade, several researchers have studied natural fiber reinforced PP composites. Joseph, V., Joseph, K., and Thomas (1999) studied the effect of sisal reinforced PP composites content on tensile strength. They have found that the tensile strength of composites increases with increasing fiber content. This is due to the fiber to matrix interaction occurring at higher fiber loading. A decrease in tensile strength with increasing fiber content has also been observed in the PP composites from kudzu, conifer, sisal and flax fiber (Luo, Benson, Kit, and Dever, 2002; Chuai, Almdal, Poulsen, and Plackett, 2001; Fung, Li, and Tjong, 2002; Liao, Huang, and Cong, 1997; Van Den Oever, Bos, and Van Kemenade, 2000; Wambua et al. 2003). In contrast, the study of sisal-PP composites has shown an increase in tensile strength with increasing fiber content (Joseph, Thomas, and Pavithrancal, 1996). However, no significant change in tensile strength with increasing fiber content has been found in the study of kenaf-PP composite (Karnani, Krishnan, and Naryan, 1997).

Gassan and Bledzki (1997) have found that the flexural strength of jute reinforced PP composite increases with increasing fiber content.

Devi, Bhagawan, and Thomas (1997) studied the mechanical properties of pineapple leaf fiber reinforced polyester composites. They have found that Young's modulus of the composites increases with increasing fiber content. An increase in Young's modulus of the composites with increasing fiber content has also been observed in PP composites from sisal, kenaf, coir, hemp, jute, and wood fiber (Joseph et al., 1999; Luo et al., 2002; Wambua et al., 2003; Coutinho, Costa, and Carvalho, 1997; Liau et al., 1997).

A decrease in elongation at break with increasing fiber content was also observed in the study of conifer-PP composites and wood-PP composites (Chuai et al., 2000; Coutinho et al., 1997). In addition, Liau et al. (1997) have found that elongation at break decreases drastically with increasing wood content in LDPE composites.

Joseph et al. (1999) studied the effect of processing variables in melt mixing method on mechanical properties of sisal reinforced PP composites by changing mixing time, rotor speed, and temperature. They have found that the optimum parameters for the sisal reinforced PP composites are as follows: mixing time of 10 min rotor sped of 50 rpm and a mixing temperature of 170^{o}C.

Joseph et al. (1996) studied the tensile strength of sisal-LDPE composites at various fiber lengths. They have found that the tensile strength of composites increases when the fiber length from 2 to 6 mm and then it decreases. This suggests a critical fiber length of approximately 6 mm for LDPE matrix. In addition, a study of flax-PP composite (Garkhail, HeijenRath, and Peijs, 2000) and sisal-PP composite (Joseph et al., 1999) have shown that tensile strength of the composites does not change when fiber length is longer than 5 mm.

2.2 The study of natural fibers reinforced composites on thermal properties

Ray, Sarkar, Basak, and Rana (2002) studied the thermal behavior of alkali treated jute fibers. Jute fiber was treated with 5 percent NaOH solution for 2, 4, 6, and 8 hours. They have found that the first peak below 100^{o}C comes from the evaporation of moisture called moisture loss peak. The peaks at 297^{o}C and 362^{o}C were caused by hemicellulose and α-cellulose degradation. For alkali treatment, the moisture loss peak shifted to a lower temperature. This is because of an increase in the surface area of the split fibers. So, it is easy to evaporate of moisture at lower temperature.

Joseph et al. (2003) studied the thermal properties and crystallization of sisal fiber reinforced PP composites using TGA and differential scanning calorimeter (DCS). They have found that the sisal fiber degraded before the PP matrix. In the case of sisal fiber, dehydration as well as degradation of lignin occur in the temperature rang 60-200^{o}C and most of the cellulose decomposed at a temperature of 350^{o}C, whereas PP decomposed at a temperature of 398^{o}C. Furthermore it was observed that the thermal stability of the sisal fiber reinforced PP composite was higher than that of the fiber and the matrix. Step analysis of neat PP thermogravimetric scan from 30 to 100^{o}C showed no mass drop whereas sisal fiber showed a mass drop of about 8%. At 200^{o}C, the mass drop of sisal fiber is about 10%. This may be attributed to the degradation of lignin in the sisal fiber. In the case of neat PP, thermal decomposition starts only at 275^{o}C. At 400^{o}C the weight loses for sisal fiber, PP and sisal reinforced PP composites are 62.92, 56.7 and 19.6, respectively. At a temperature of around 500^{o}C, PP is completely decomposed. Moreover, it was shown that the degradation

temperature is shifted to a slightly higher region in the case of treated composites than that of untreated composite. Calorimetric investigations showed that the incorporation of sisal fiber in PP caused an apparent increase in the T_c and percentage of crystallinity. These effects can be attributed to the fact that the surfaces of sisal fiber act as nucleating sites for the crystallization of the polymer, promoting the growth and formation of transcrystalline regions around the fiber. Similarly, Wielage, Lampke, Marx, Nestler, and Starke (1999) studied thermal properties of flax, hemp, and polypropylene by TGA and DSC.

Varma et al. (1987) studied the thermal behavior of jute fibers. They have reported that there was an approximate 2.5-3.5% weight loss up to 150^{o}C in jute fiber, which can be attributed to desorption of physically adsorbed water. Major weight loss in this fiber occurred above 200^{o}C. Initially the rate of weight loss was slow, but above 300^{o}C the rate increased considerably in both air and nitrogen atmosphere. When degradation in air was done, the decomposition proceeded in three steps. The first step started losing weight above 350^{o}C, and nearly complete weight loss occurred at 500^{o}C. Thermal degradation of cellulose is following steps of temperature: (a) physical desorption of monomolecularly adsorbed water (25-150^{o}C), (b) dehydration from the cellulose unit (150-240^{o}C), (c) thermal cleavage of glycosidic linkage by transglycosylation and scission of other C-O and C-C bonds (240-400^{o}C), and (d) aromatization (>400^{o}C) involving dehydrogenation reactions. When adding coupling agents, the weight loss decreases in the region 50-150^{o}C. It indicated that all of treatments have imparted moisture repellency to the fibers. Also the same result of the thermal stability of acetylated sisal fibers was studied by Albano, Gonzalez, Ichazo, and Kaiser (1999).

Amash and Zugenmaier (2000) have studied the morphology and properties of isotropic and oriented samples of cellulose fiber PP composites. They have found that no significant change in the melting temperature at various cellulose contents in PP composites. In addition Manchado, Biagiotti, Torre, and Kenny (2000) have studied the effect of reinforcing fibers on the crystallization of PP. They have shown that sisal fiber has no effect on the melting temperature of PP composites.

Zafeiropoulos, Baillie, and Matthews (2001) have observed two small peaks on DSC curve of flax-PP composite, which indicates different morphology in the composites.

Quillin, Yin, Koutsky, and Caulfield (1994) have found that the addition of cellulose fiber to PP results in increasing crystallization temperature of the polymer matrix due to cellulose fibers acting as a nucleating agent for the crystallization of PP.

2.3 The study of interface modifications on natural fibers reinforced composites

In natural fiber reinforced polymer composites, there is a lack of interfacial adhesion between the hydrophilic cellulose fibers and the hydrophobic resin due to their inherent incompatibility (Saheb and Jog, 1999). As a result, it has poor resistance to moisture absorption and poor mechanical properties. This made the use of natural fiber reinforced composite less attractive. This problem can be improved by choosing the method to modify or treat natural fiber with suitable chemical.

2.3.1 Graft copolymerization

This reaction is initiated by free radicals of the cellulose molecule. The cellulose is treated with an aqueous solution with selected ions and is exposed to high-energy radiation. Then the cellulose molecules crack and radicals are formed. After that the radical sites of the cellulose are treated with a suitable solution for example vinyl monomer, acrylonitrile and methyl methacrylate. After treatment the surface energy of the fibers is increased to a level much closer to the surface energy of the matrix. Thus, a better wettability and a higher interfacial adhesion can be obtained (Rana, Mandal, Mitra, Jacobson, Rowell, and Banerjee, 1998; Mishra, Naik, and Patil, 2000)

Mishra, Misra, Tripathy, Nayak, and Mohanty (2001) studied graft copolymerization of acrylonitrile on chemical modified sisal fiber. They have found that the tensile strength of sisal fiber is higher than that of untreated fiber.

Saha, Das, Basak, Bhatta, and Mitra (2000) studied the mechanical properties of jute fiber based composites by acrylonitrile treatment. They have reported that the tensile strength and flexural strength of the composites with acrylonitrile treated fiber are higher than that of untreated fiber.

Chuai et al. (2001) studied the effect of maleic anhydride (MA) on mechanical properties of conifer fiber reinforced PP composites. They have found that the tensile strength of conifer fiber reinforced PP composites with MA is higher than untreated fiber. The notch impact strength of MA treated fiber is higher than that of untreated fiber.

Similarly, many researchers have shown that the mechanical properties of PP composites from sisal, jute, kudzu, flax, and kenaf fiber can be improved by

using maleic anhydride grafted PP (Joseph et al., 2003; Fung et al., 2002; Gassan and Bledzki, 1997; Luo et al., 2002; Cantero, Arbelaiz, Llano-Ponte, and Mondragon, 2003; Sanadi, Caulfield, Jacobson, and Rowell, 1995; Mieck, Nechwatal, and Knobelsdorf, 1995, quoted in Gassan and Bledzki, 1999).

2.3.2 Alkali treatment

Alkali treatment is the mercerization of cellulose which is the process of subjecting a vegetable fiber to an interaction with a fairly concentrated aqueous solution of a strong base, to produce great swelling with resultant changes in the fine structure, dimension, morphology and mechanical properties. The objective of the alkali treatment of fiber surface is to remove the surface impurities as lignin wax and oil, the swelling of crystalline region and removal the hydrophilic hydroxyl groups. NaOH is the mostly used chemical for cleaning the surface of fiber. (Li, Mai, and Ye, 2000; Mwaikambo and Ansell, 1999)

Ray and Sarkar (2001) studied the effect of alkali treatment of jute fiber on mechanical properties. They treated jute fibers with 5 percent concentration of NaOH solution for 0, 2, 4, 6, and 8 hours. The hemicellulose content of the jute fibers was reduced with increasing treatment time but the α-cellulose was unchanged by alkali treatment. The tenacity of the fibers which is a measure of specific stress at break drops after an initial 2 hours of treatment. The percent strain at break point of the fibers decreased from 1.16 to 0.89 for 8 hours treated fibers. This is due to the fiber becoming more brittle. The most of changes in mechanical properties occurred within 2 to 4 hours of alkali treatment. The change has maximum at 4 hours of treatment. This is because the heavy loss of hemicellulose as a cementing constituent in the first region to 4 hours of treatment contributed to the closer packing of the

cellulose chains, leaving the fibrils with the freedom for reorientation along the direction of the tensile force. The large loss of hemicellulose made the fibers lose their cementing capacity. Then the fiber can separate out from each other.

Similarly, many researchers have reported that NaOH treatment on jute, sisal, hemp, and oil palm fibers can partially remove the hemicellulose, waxes and lignin present on the surface of fiber. (Sydenstricker, Mochnz, and Amico, 2003; Razerra and Frollini, 2004; Lu, Zhang, Rong, Shi, and Yang, 2003; Mishra et al., 2001; George, Sreekala, and Thomas, 2001; Iannace, Ali, and Nicolais, 2001; Mwaikambo and Ansell, 1999).

Joseph et al. (1996) studied the effect of alkali treatment on the tensile properties of short sisal fiber reinforced polyethylene (PE) composites They have found that the tensile strength of alkali treated sisal fiber is higher than that of untreated fiber. This is similar to the results from the studies of the sisal-PP composites studied by Joseph et al. (1999). They have found that the alkali treatment enhanced the mechanical properties of the composites. An improve in mechanical properties of the composites with alkali treatment has also been observed in sisal-epoxy composite and jute-epoxy composites (Rong, Zhang, Liu, Yang, and Zeng, 2001; Gassan and Bledzki, 1999)

2.3.3 Organosilanes as coupling agents treatment

Organosilanes are the main group of coupling agents for fiber reinforced polymers composite. Most of the silane coupling agents can be represented by the following formula: $R - 2\ (CH_2)_n - Si\ (OR')_3$ where n = 0–3, OR′ is the hydrolyzable alkoxy group . Where as R is an organo functional group which can chemically react with the matrix. R′ is usually a methyl or ethyl group. The curing

reaction of a silane treated substrate enhances the wetting ability by the matrix resin. (Kinloch, 1986; Rong et al., 2001; Mwaikambo and Ansell, 1999; Plueddemann, 1982).

Herrera-Franco and Aguilar-Vega (1997) studied the effect of fiber treatment by using silane on the mechanical properties of LDPE henequen cellulose fiber composites. They have found that the fiber surface treatment as silane coupling agent can improve the tensile strength of the composites compared to untreated fiber.

Valadez-Gonzalez, Cervantes-Uc, Olayo, and Herrera-Franco (1999) studied the effect of silane treatment on henequen fiber reinforced composites. They have found that the tensile strength of the silane treatment on fiber in composites is higher than that of untreated fiber. This is because the silane used to modify the fiber has two functional groups. There are hydrolyzable alkoxy group able to condense with hydroxyl of henequen surface fiber and an organofunctional (vinyl) group able to interacting with the thermoplastic matrix.

Similarly, several authors have reported that the silane treatments improve the mechanical properties of kenaf-PP composites, sisal-PP composite, and wood-linear low density polyethylene (LLDPE) (Joseph et al., 1999; Karnani et al., 1997; Liao et al., 1997).

2.3.4 Isocyanates treatment

Joseph, et al. (1996) studied the effect of isocyanate treatment on the tensile properties of short sisal fiber reinforced polyethylene (PE) composites. They have found that the tensile strength and modulus of cardanol derivative of toluene dissocyanate (CTDIC) treated fiber composites is higher than that of untreated fiber reinforced composites.

2.3.5 Acetylation treatment

Rong et al. (2001) studied the tensile strength of acetylation on sisal fiber reinforced epoxy composites. The tensile strength of acetylated sisal fiber reinforced epoxy composites is slightly higher than that of untreated fiber.

Ichazo, Albano, and Gonzalez (2000) studied the behavior of polyolefins blends with actylated sisal fibers. They have found that the tensile strength of treated sisal fiber is higher than that of untreated sisal fiber reinforced polyolefins composites.

2.4 The study of the environmental effects on properties of natural fibers reinforced composites

During service, polymeric materials are subjected to a variety of environmental conditions such as moisture, solvents, oil, temperature, mechanical loads and radiation. Moisture effects in fiber reinforced polymer composites have been studied widely during the last two decades. This effect can be minimized by using suitable modifications.

2.4.1 The effect of fiber loading on water absorption

Joseph , Rabello, Mattoso, Joseph, and Thomas (2002) studied the effect of fiber loading on water absorption. They have found that the initial rate of water absorption increases with increasing fiber contents. The increasing in water absorption is due to the higher hydrophilic nature of sisal fiber in the composites. An increase in water absorption with increasing fiber loading was also observed in the study of pineapple-PE composites and wood-LDPE composites (George, Bhagawan,

and Thomas, 1998; Ichazo, Albano, Gonzalez, Perera, and Candal, 2001). Moreover, Mishra et al. (2000) observed the effect of water absorption of the banana, hemp and sisal fiber reinforced novalac resin. They have reported that the percent water absorption increases with increasing fiber loading.

2.4.2 The effect of chemical treatment on water absorption

George et al. (1998) studied the effect of chemical treatments on pineapple fiber reinforced LDPE composite. They have found that the chemical treatment e.g isocyanate, silane, NaOH on pineapple fiber in composites show lower water absorption than that of untreated fiber in composites.

Mishra et al. (2000) studied the effect of water absorption of the banana, hemp and sisal fiber reinforced novalac resin by treated MAPP at ambient temperature for 30 hours. They have shown that the water absorption of untreated fiber is higher than that of the MA treated fiber.

Gassan and Bledzki (1997, quoted in Gassan and Bledzki, 1999) studied the silane treatment on jute fiber reinforced composite. They have found that moisture of the composites with silane treated jute fiber is lower than that of untreated jute fiber. Similarly, Bisanda and Ansell (1991, quoted in Li et al., 2000) have found that silane treatment improves the wettability of sisal fiber reinforced epoxy composite.

In addition, Mishra et al. (2001) studied the graft copolymerization of acrylonitritrile on sisal fiber. They have found that the water absorption of the treated fiber is lower than that of untreated fiber. Similarly, Bisanda (2000) has found that the water absorption of the alkali treated sisal fiber reinforced epoxy composites is lower than that of untreated fiber

Moreover, Singh, Gupta, Verma, and Tyagi (2000) investigated the effect of chemical treatments as N-substituted methacrylamide on sisal fiber reinforced unsaturated polyester. They have found that the composites prepared from treated fiber absorb less water than that of composites prepared from untreated fiber.

2.4.3 The effect of radiation on properties of natural fibers reinforced composites

Joseph et al. (2002) studied the degradation behavior of sisal fiber reinforced PP composite by UV radiation. They have reported that the tensile strength decreases with increasing the time exposure to UV radiation. The reduction in properties was due to chain scission and degradation on PP molecule during irradiation for a longer duration. The tensile strength of the treated fiber is higher than that of untreated fiber.

CHAPTER III

EXPERIMENTAL

3.1 Materials

A commercial grade of isotactic PP (700J) with density of 0.910 g/cm^3 was supplied by Thai Polypropylene Co., Ltd. Vetiver grass (*Vetiveria zizanioides*) was obtained from The Land Development Department, Nakhon Ratchasima, Thailand. The picture of vetiver grass is shown in Figure 3.1. In this research, vetiver leaves with length of 30 cm from vetiver culm were used. The ages of vetiver grass are around 6-8 months. Sodium hydroxide (NaOH) laboratory grade obtained from Merck was used. Vinyltrimethoxy silane (A-171) coupling agent obtained from Optimal Tech Co., Ltd was used.

Figure 3.1 Vetiver grass (*Vetiveria zizanioides*).

3.2 Sample preparations

3.2.1 Vetiver grass preparations

First, vetiver leaves were washed by water to get rid of dirt and then were dried by sunlight for one day. To prepare vetiver leaves (VL), the washed vetiver leaves were ground by the Retsch grinder machine. VL were sieved to obtain the average length of 2 mm. The average length of VL was measured by using a Nikon polarized optical microscope (model Eclipes E600 POL). The average lengths of VL length were calculated based on 100 samples.

To prepare NaOH treated vetiver leaves (NaOH-VL), the VL were immersed in 1% (w/v) NaOH solution for 5 days, washed by water, and dried in an oven at 100^{o}C for 6 hours. Then, it was ground by a Retsch grinder machine. NaOH-VL was prepared into 3 different lengths; 0.10 mm, 2 mm, and 4 mm. The average length of NaOH-VL was measured by using a Nikon polarized optical microscope (model Eclipes E600 POL). The average lengths of NaOH-VL were calculated based on 100 samples.

To obtain vetiver fibers (VF), the VL were immersed in 1% (w/v) NaOH solution for 5 days, washed by water, and brushed to obtain the vetiver fibers from the leaves. After that, VF were cut into the length of 2 mm by using scissors. The VL, NaOH-VL, and VF were dried in an oven at 100^{o}C for 6 hours.

To prepare NaOH treated VF (NaOH-VF), the VF were immersed in 5% (w/v) NaOH solution at various time e.g. 2, 4, 6 hours. NaOH-VF were washed by water to remove NaOH left on vetiver fiber and then NaOH-VF were dried in an oven at 100^{o}C for 6 hours.

To prepare NaOH silane vetiver fiber (NaOH-silane-VF), the VF were immersed in 5% (w/v) sodium hydroxide solution for 4 hours then they were washed by water and dried in an oven at 100^{o}C for 6 hours. After that they were immersed in 2% (w/v) vinyltrimethoxysilane (A-171) for 1 hour. The pH of the solution was adjusted to 3.5 with acetic acid and stirred continuously during 10 min. Then, the NaOH-silane-VF were washed by water and dried in an oven at 100^{o}C for 6 hours. A summary of abbreviation of vetiver grass from various treatments used in this study are shown in Table 3.1.

Table 3.1 Summary of abbreviation of vetiver grass from various treatments.

Abbreviation	Surface treatment
VL	Vetiver leave
NaOH-VL	Vetiver leave treated with NaOH solution
VF	Vetiver fiber
NaOH-VF	Vetiver fiber treated with NaOH solution
NaOH-silane-VF	Vetiver fiber treated with NaOH solution and then with a silane coupling agent

3.2.2 Vetiver-PP composites preparations

3.2.2.1 Mixing procedures

Vetiver-PP composites were prepared by two different mixing procedures, method A and method B.

Method A

Vetiver grass was added after PP was melted for 5 min in an internal mixer (model Hakke Rheomix Polylab) and the mixing time after adding vetiver grass was 5 min at 170^{o}C with a rotor speed of 50 rpm. Then, the mixtures were ground by a plastic recycling machine. The ratios of vetiver grass were varied from 5%, 10%, 20%, 30%, and 50% by weight.

Method B

Vetiver grass and PP were mixed together for 10 min in an internal mixer (model Hakke Rheomix Polylab) at 170^{o}C with a rotor speed of 50 rpm for 10 min.

3.2.2.2 Specimen preparations

The composite specimens both impact and tensile were prepared by injection molding using a Chuan Lih Fa injection machine (model CLF 80P) with melt temperature at 170^{o}C, mold temperature at 15^{o}C, injection speed of 46 cm^3/sec, injection pressure of 960 kg/cm^2, and holding pressure of 640 kg/cm^2. A photograph of the PP specimen is shown in Figure 3.2.

Figure 3.2 The PP specimen from injection molding.

3.3 Material characterizations

3.3.1 Physical properties

The density of VF was determined using a specific gravity bottle with p-xylene as the fluid.

The diameter of VF was measured using a Nikon polarizing optical microscope (model Eclipes E600 POL).

Tensile properties of VF were examined using an Instron universal testing machine (model 4502) with a crosshead speed of 120 mm/min and a gauge length of 100 mm.

The chemical compositions of VL, NaOH-VL, and VF were obtained from X-Ray Fluorescence Spectrometer (model ED 2000).

3.3.2 Thermal properties

Thermal analysis of vetiver grass was determined using TA thermogravimatric analysis (model SDT 2960). Thermal analysis of vetiver-PP composites was determined using TA thermogravimatric analysis (model SDT 2960)

and Perkin Elmer Instruments differential scanning calorimetry (model DSC-7). TGA curves of vetiver grass and vetiver-PP composites were obtained by heating the sample from 30-600^{o}C under a nitrogen atmosphere and switch over to an oxygen atmosphere from 600-800^{o}C at heating rate of 10^{o}C/min. The sample weight of each material is between 5-10 mg. DSC curves of vetiver-PP composites were obtained in 3 steps. The first heating scan was performed by heating the sample from 25^{o}C to 200^{o}C and annealed for 5 min to remove the thermal history. After that the cooling scan was begun. The sample was then cooled to 25^{o}C at a cooling rate of 10^{o}C/min in a nitrogen atmosphere. Finally, the second heating scan was done by heating the sample from 25^{o}C to 200^{o}C at heating rate of 10^{o}C/min in a nitrogen atmosphere. The baseline of the heating and cooling process was done by placing empty pans in both the reference and sample compartments of the DSC. The baseline was later subtracted from the experimental heat flow curve. The sample weight of each material was cut from tensile specimen between 5-10 mg.

The crystallinity of vetiver-PP composites was calculated by the following equation:

$$\% \text{ Crystallinity} = (\Delta H_{\text{sample}} / \Delta H_{100\% \text{ crystalline}}) \times 100 \quad (1)$$

where ΔH_{sample} is the heat of fusion of sample (J/g).

$\Delta H_{100\% \text{ crystalline}}$ is the heat of fusion of pure crystalline.

In case of PP, the $\Delta H_{100\% \text{ crystalline}} \approx 207.1$ J/g as referred by Krevelen, (1997).

3.3.3 Rheological properties

Melt flow index (MFI) of vetiver-PP composites was obtained using a Kayeness melt flow indexer at 170^{o}C with a load cell of 2.160 kg and melt time at 360 sec.

Shear viscosity at the shear rate range of 10 to 1000 s^{-1} of vetiver-PP composites was measured using the Kayeness capillary rheometer at 170^{o}C.

3.3.4 Mechanical properties

Tensile properties of vetiver-PP composites were examined using an Instron universal testing machine (model 5565) with a load cell of 5 kN, a crosshead speed of 10 mm/min and a gauge length of 80 mm. Ten specimens were used in each experiment. The tensile strength of PP was obtained by using a test speed at 50 mm/min. This is because PP specimen does not break at a speed of 10 mm/min.

Izod type impact tests of the unnotched composites samples were studied using an Atlas testing machine (model BPI).

HDT of vetiver-PP composites was investigated using HDT testing machine (model HDV 1 Manual DTVL/VICAT) at a heating rate of 120^{o}C/hour at 455 KPa.

3.3.5 Morphological properties

The surface morphological of vetiver grass and the fracture surface of the composites specimens obtained from unnotched Izod specimens from impact testing were studied using SEM (model JSM 6400) at 5 keV. Fracture surface was coated with gold for about 3 min.

The shear-induced crystallization of vetiver-PP composites specimens was obtained from tensile specimens. The samples were cut perpendicular to the flow direction (MD) and parallel to the transverse direction (TD) at various distances from the gate using an electric sawing machine (Jaespa AS 4). Each of these pieces was cut through the center plane parallel to MD using surgical blade. Then a microtome, RMC MT 960, was used to cut into thin film with the thickness of 30 μm from the

midplane in parallel to MD. The thickness of skin layer was measured by Nikon polarized optical microscope (model Eclipes E600 POL).

The normalized thickness (%) of skin layer of vetiver-PP composites was calculated by dividing the skin thickness of polymer sample by the total thickness of test specimen as shown in equation (2).

Normalized skin thickness = (Skin thickness / Total thickness of test specimen) x 100 (2)

CHAPTER IV

RESULTS AND DISCUSSION

4.1 Physical and mechanical properties of vetiver grass

The physical and mechanical properties of VF are shown in Table 4.1. These properties are in the same range as those of other natural fibers shown in Table 4.2. The density of VF is in the same range as flax and ramie. The tensile strength of VF is higher than that of coir fiber. Young's modulus of VF is higher than that of cotton, sisal, and coir but it is lower than that of jute, flax, and ramie. Elongation at break of VF is higher than that of jute fiber.

Table 4.1 Physical and mechanical properties of VF.

Properties	VF
Density (g/cm^3)	1.5
Diameter (μm)	100-220
Tensile strength (MPa)	458.4
Young's modulus (GPa)	23.2
Elongation at break (%)	2.1

Table 4.2 Physical properties of some natural fibers (Bledzki and Gassan, 1999).

Fiber	**Density (g/cm^3)**	**Diameter (μm)**	**Tensile strength (MPa)**	**Young's modulus (GPa)**	**Elongation at break (%)**
Cotton	1.5-1.6	-	287-800	5.5-12.6	7.0-8.0
Jute	1.3-1.4	25-200	393-773	13.0-26.5	1.1-1.5
Flax	1.5	-	345-1100	27.6	2.7-3.2
Ramie	1.5	-	400-938	61.4-128.0	1.2-3.8
Sisal	1.4	50-200	468-640	9.4-22.0	3.0-7.0
Coir	1.1	100-450	131-175	4.0-6.0	15.0-40.0

The chemical compositions of VL, NaOH-VL, and VF obtained from X-ray fluorescence spectrometer are shown in Table 4.3. These include organic and inorganic compositions. There are many inorganic compositions in the structure of vetiver grass e.g., SiO_2, K_2O, P_2O_5. The highest amount of inorganic composition is SiO_2. In addition, VL shows the highest amount of SiO_2 compared to NaOH-VL and VF.

Table 4.3 Chemical compositions of VL, NaOH-VL, and VF.

Chemical compositions	**VL (% wt)**	**NaOH-VL (% wt)**	**VF (% wt)**
C	89.39	97.30	99.00
SiO_2	5.74	1.17	0.34
K_2O	3.34	0.21	0.02
P_2O_5	0.33	0.12	0.03
SO_3	0.28	0.05	0.02
Al_2O_3	0.14	0.05	0.02
MgO	0.07	0.07	0.07
Cl	0.07	0.02	0.01
MnO	0.05	0.04	0.02
Na_2O	0.00	0.01	0.00
Others*	0.10	0.07	0.01

* See Appendix B

4.2 Thermal properties of vetiver grass and vetiver-PP composites

4.2.1 The effect of chemical treatment on thermal properties of vetiver grass

TGA and DTG curves of VL, NaOH-VL, VF, and NaOH-silane-VF are shown in Figure 4.1. All TGA curves show the initial transition around 100°C due to the moisture evaporation. The moisture content about 3% is observed. The decomposition temperature of VL around 174°C may be caused by the loss of low molecular weight compositions, e.g., wax. In case of NaOH-VL, VF, and NaOH-silane-VF, this decomposition temperature of low molecular weight compositions is not observed. This indicates that NaOH removes the low molecular weight components from vetiver leaves. The decomposition temperature of hemicellulose of VL, NaOH-VL, VF, and NaOH-silane-VF are around 310°C, 311°C, 312°C, and 312°C, respectively. There is no significant difference in hemicellulose decomposition temperature of VL, NaOH-VL, VF, and NaOH-silane-VF. In addition, the decomposition temperatures of α-cellulose of NaOH-VL, VF, and NaOH-silane-VF are around 348°C, 346°C, and 343°C, respectively. In case of VL, the decomposition temperature of -cellulose can not be observed as a peak in DTG curves. However, the beginning of decomposition temperature can be observed around 333°C from DTG curves. The decomposition temperatures of hemicellulose and -cellulose of vetiver grass are in the same range as those of jute, hemp, and sisal (Ray et al., 2002; Albano et al., 1999; Joseph et al., 2003). The residue weight of VL left around 800°C is higher than that of NaOH-VL, VF, and NaOH-silane-VF. This may be due to the inorganic compositions in the grass, especially silica as shown in Table 4.3.

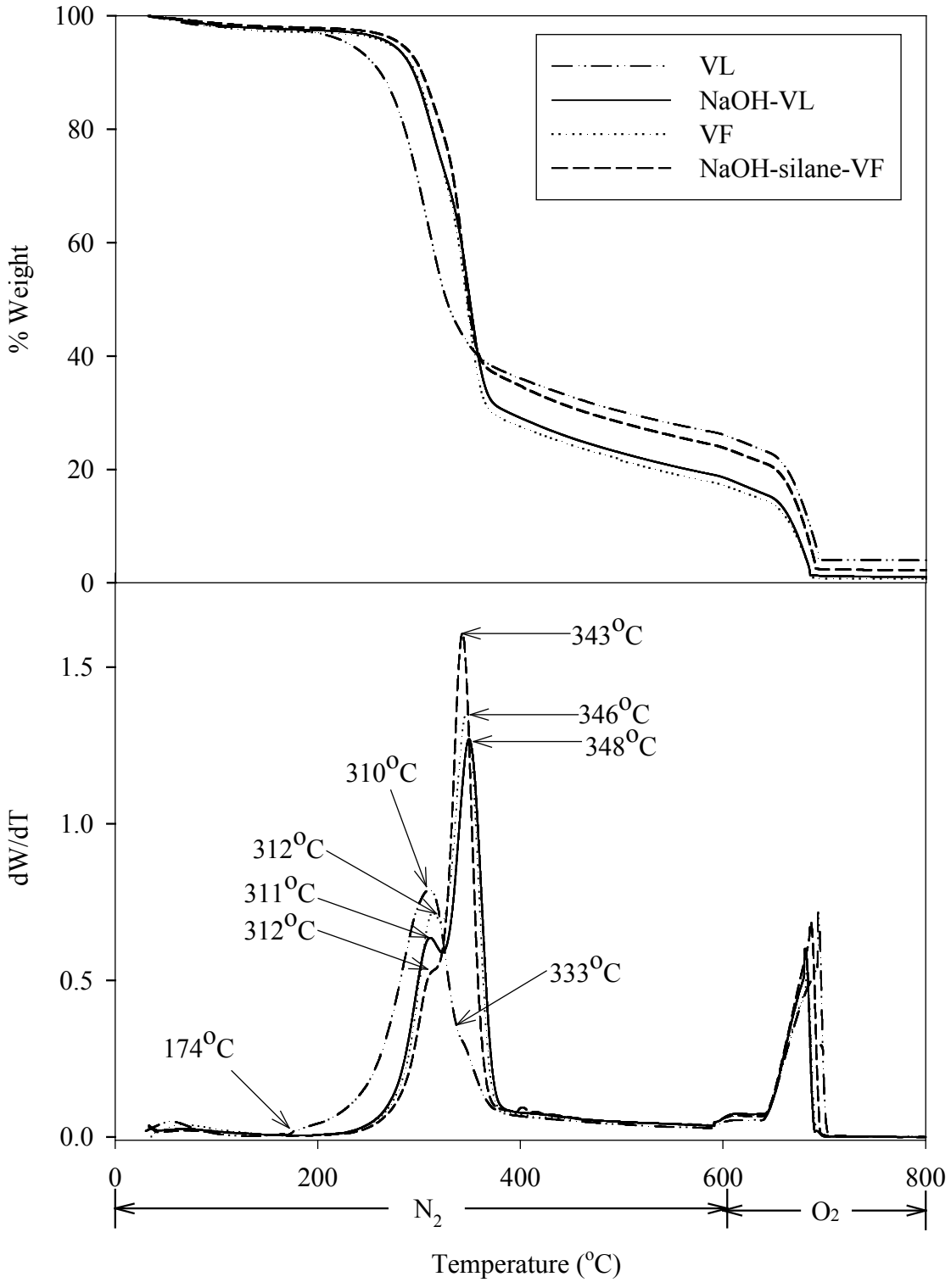

Figure 4.1 TGA and DTG curves of VL, NaOH-VL, VF, and NaOH-silane-VF.

4.2.2 The effect of vetiver content on thermal properties of vetiver-PP composites

TGA and DTG curves of PP and VF-PP composites at 5%, 10%, 20%, and 30% vetiver contents are shown in Figure 4.2.At hi gher percent of vetiver contents, the higher amount of moisture can be observed. The decomposition temperature of PP is at 445^{o}C and PP completely decomposes around 500^{o}C. The decomposition temperatures of hemicellulose (308^{o}C-310^{o}C) and α-cellulose (352^{o}C-353^{o}C) can be observed when the vetiver content is increased from 10% to 20% and 30%. The decomposition temperature of α-cellulose of the composite is higher than that of VF. This is because PP matrix inhibits the decomposition of -cellulose. The beginning of decomposition of the composites decreases with decreasing PP content due to the low thermal stability of vetiver grass.

DSC curves of the PP and vetiver-PP composites from VF at various vetiver contents obtained from the first heating scan, the cooling scan, and the second heating scan are shown in Figure 4.3-4.5, respectively. The first heating curves of PP show a single peak of melting temperature while that of vetiver-PP composites show two small peaks of melting temperature. These two small peaks can be possibly attributed to a slightly different morphology of the matrix or various forms of crystal formed during processing. These different forms of crystal disappear after removing the thermal history as shown by the narrow melting peak in the second heating curve. Similarly, Zafeiropoulos, et al. (2001) have observed two small peaks on DSC curve of flax-PP composite, which indicates different morphology in the composites.

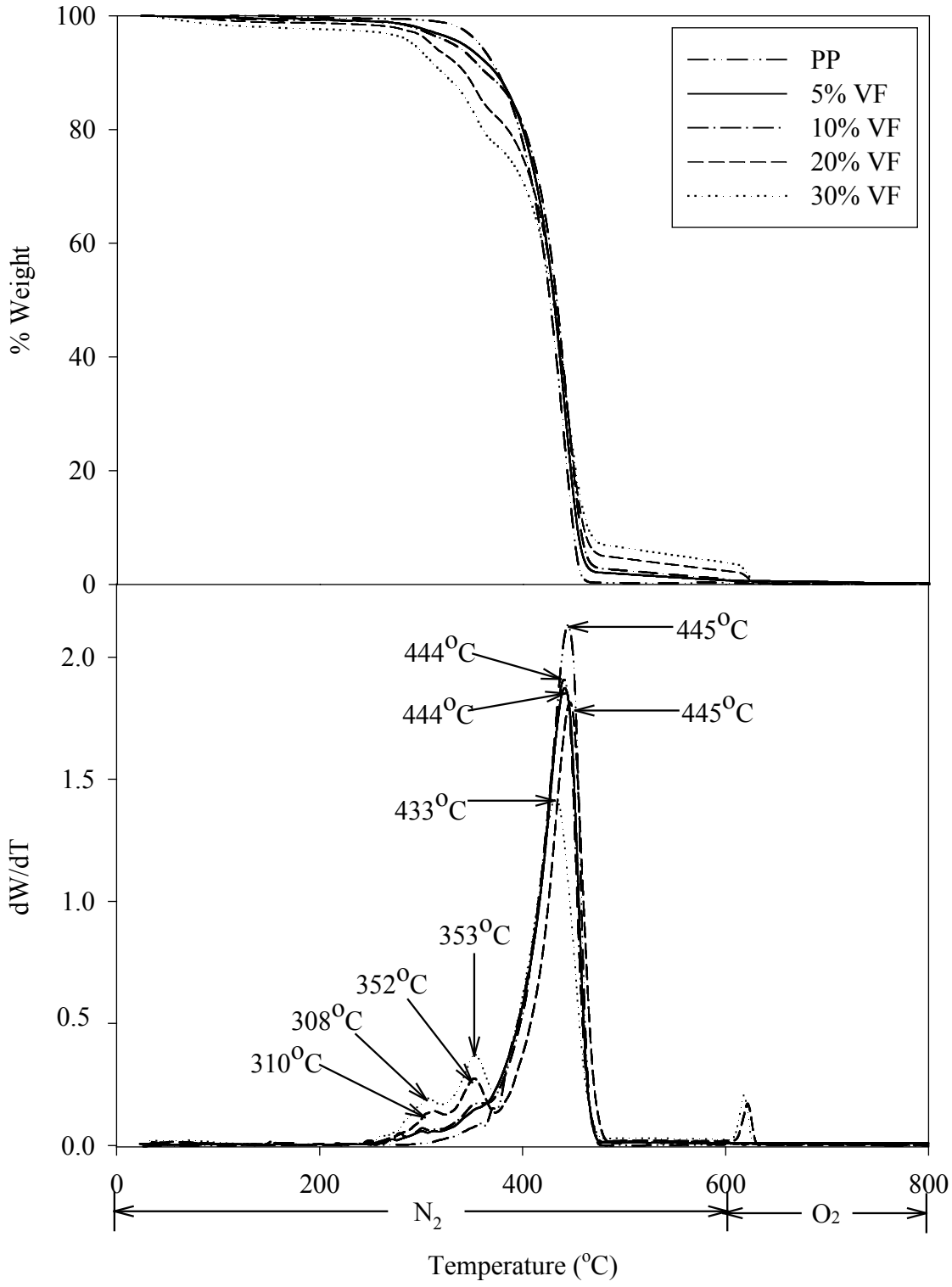

Figure 4.2 TGA and DTG curves of PP and VF-PP composites at 5%, 10%, 20%, and 30% vetiver contents.

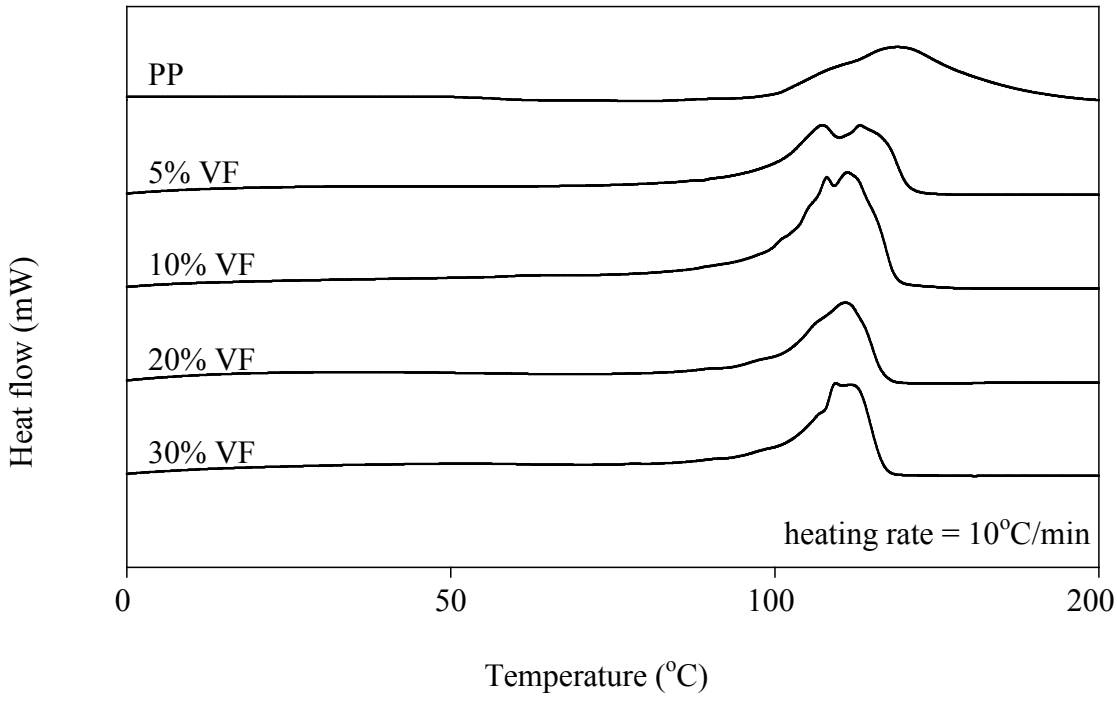

Figure 4.3 DSC curves corresponding to the first heating scans of PP and VF-PP composites at 5%, 10%, 20%, and 30% vetiver contents.

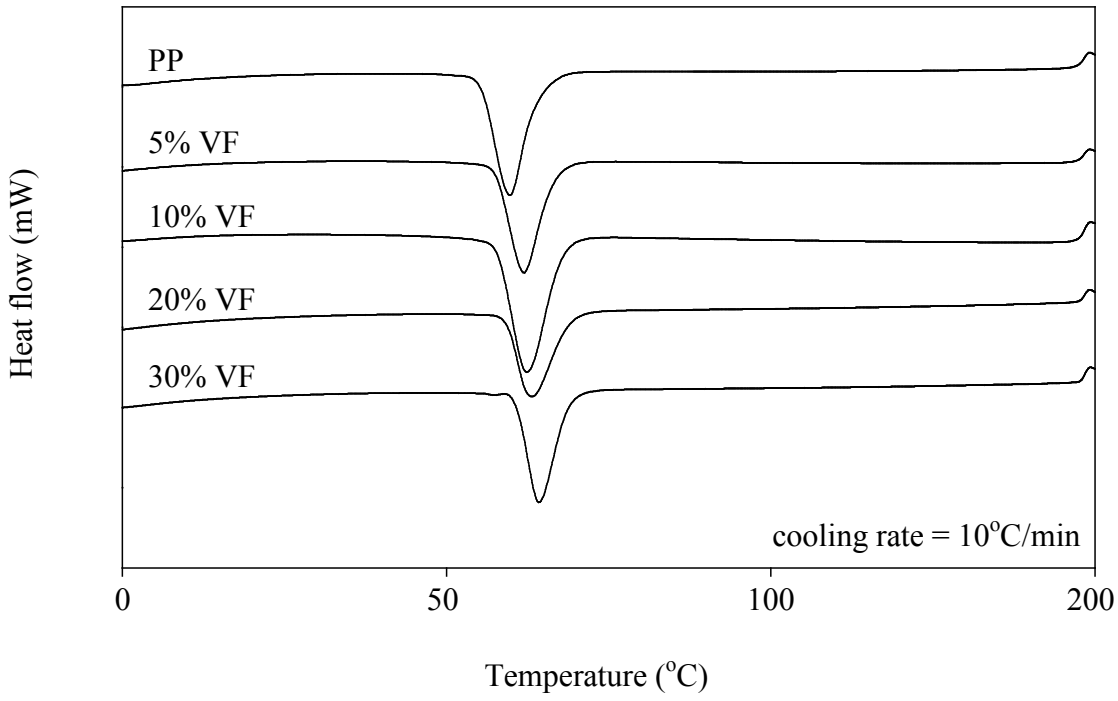

Figure 4.4 DSC curves corresponding to the cooling scans of PP and VF-PP composites at 5%, 10%, 20%, and 30% vetiver contents.

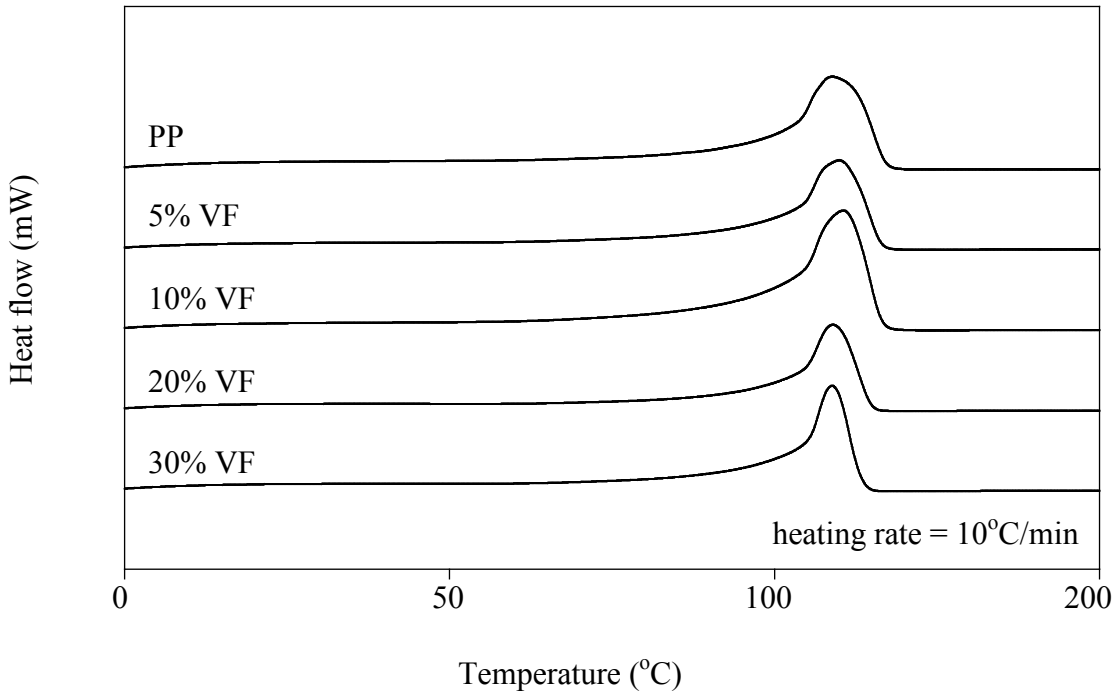

Figure 4.5 DSC curves corresponding to the second heating scans of PP and VF-PP composites at 5%, 10%, 20%, and 30% vetiver contents.

The values of the melting temperature obtained from the second heating scans in Figure 4.5 are shown in Table 4.4. It shows no significant change in melting temperature of vetiver-PP composite with increasing vetiver contents. Similarly, Amash and Zugenmaier (2000) have studied the morphology and properties of isotropic and oriented samples of cellulose fiber PP composites. They have found no significant change in the melting temperature at various cellulose contents in PP composites. In addition, Manchado et al. (2000) have studied the effect of reinforcing fibers on the crystallization of PP. They have shown that sisal fiber has no effect on the melting temperature of PP composites. The values of % crystallinity and crystallization temperature calculated from Figure 4.3 and Figure 4.4, respectively,

are shown in Table 4.5. The crystallization temperature of vetiver-PP composites slightly increase with increasing vetiver contents. Moreover, the % crystallinity slightly decrease with increasing vetiver contents. This can be explained as follow; the crystallization process is governed by nucleation and crystal growth. The vetiver fibers act as a nucleating agent for the crystallization in the nucleation step. This results in increasing crystallization temperature. After nucleation, the presence of vetiver fiber may restrict the molecular mobility in the melt resulting in lower % crystallinity with increasing vetiver content. In addition, Amash and Zugenmaier (2000) and Quillin et al. (1994) have found that the addition of cellulose fiber to PP results in increasing crystallization temperature of the polymer matrix due to cellulose fibers acting as a nucleating agent for the crystallization of PP.

Table 4.4 Melting temperature of vetiver-PP composites from VF at various vetiver contents from the second heating scans.

Vetiver content (% wt)	**Melting temperature (^{o}C)**
0	159
5	159
10	160
20	159
30	159

Table 4.5 Crystallization temperature and % crystallinity of vetiver-PP composites from VF at various vetiver contents.

Vetiver content (% wt)	**Crystallization temperature (^oC)**	**% Crystallinity (X_c)**
0	109	45.1
5	111	44.7
10	112	44.4
20	113	37.8
30	114	33.7

4.2.3 The effect of chemical treatment on thermal properties of vetiver-PP composites

TGA and DTG curves of vetiver-PP composites from VL, NaOH-VL, VF, and NaOH-silane-VF at 20% vetiver content are shown in Figure 4.6. The TGA curves show the initial transition around 100^{o}C due to the moisture evaporation. The decomposition temperatures of -cellulose of the composites from NaOH-VL, VF, and NaOH-silane-VF are in the same range (351^{o}C-353^{o}C), which are higher than those of NaOH-VL, VF, and NaOH-silane-VF (343^{o}C-348^{o}C). Nevertheless, the decomposition of α-cellulose of the composite from VL is not observed. The beginning decomposition temperature of the composite from VL is lower than those of the composites from NaOH-VL, VF, and NaOH-silane-VF. This is due to the lower thermal stability of VL.

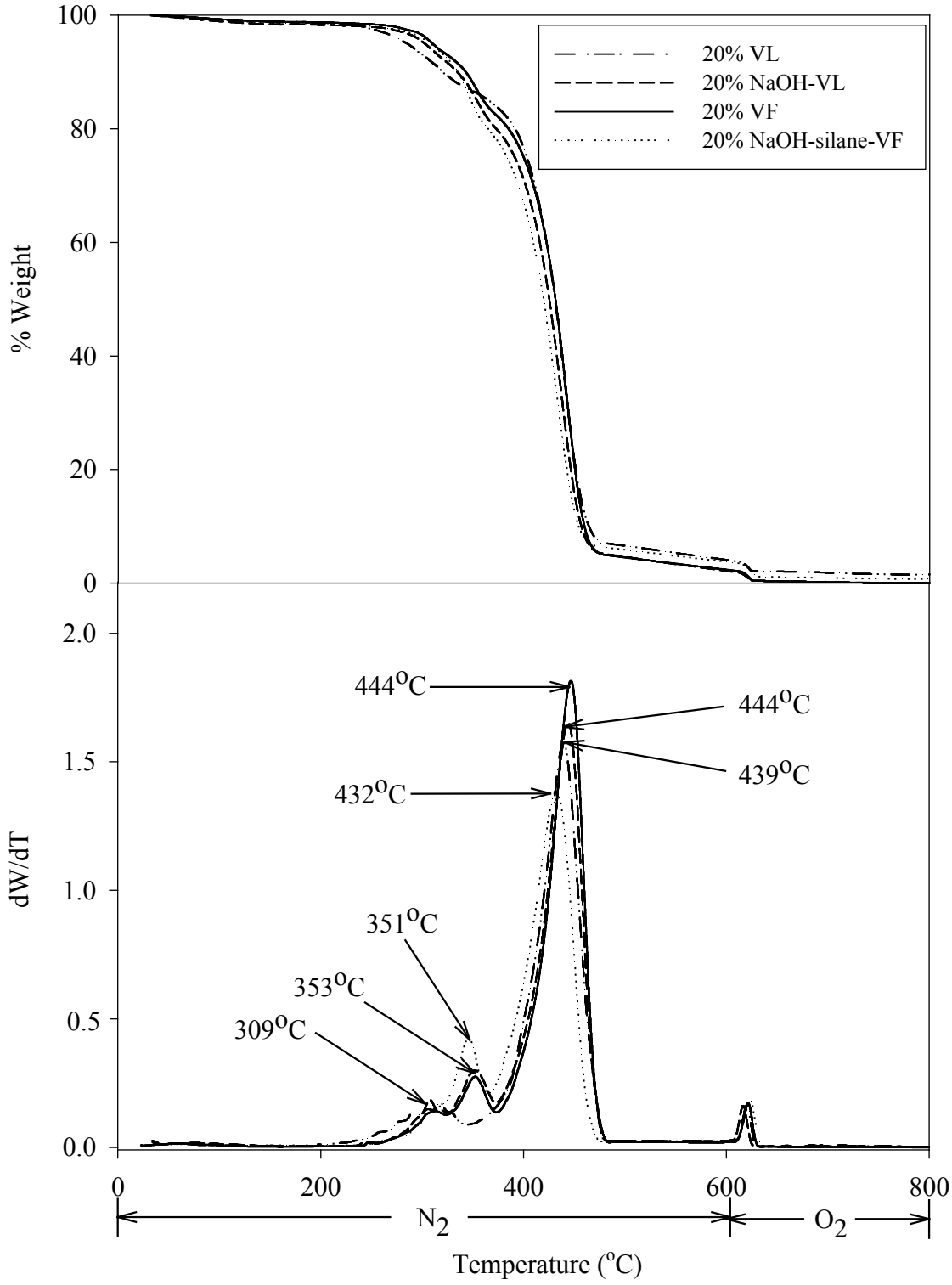

Figure 4.6 TGA and DTG curves of vetiver-PP composites from VL, NaOH-VL, VF, and NaOH-silane-VF at 20% vetiver content.

DSC curves of PP composites from VL, NaOH -VL, VF, and NaOH-silane-VF at 20% vetiver content obtained from the first heating scan, the cooling scan, and the second heating scan are shown in Figure 4.7-4.9, respectively. The first heating curves show several small peaks of melting temperature, which may indicate various forms of crystal formed during processing. These different forms of crystal disappear after removing the thermal history as shown by the single melting peak in the second heating scans.

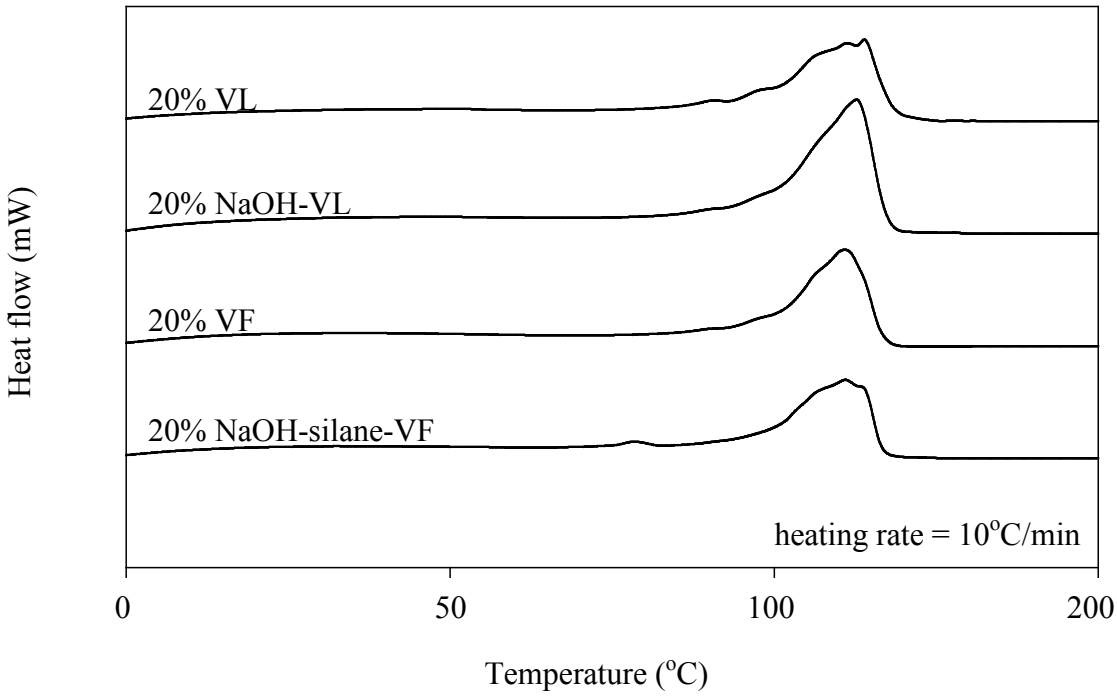

Figure 4.7 DSC curves corresponding to the first heating scans of vetiver-PP composites from VL, NaOH-VL, VF, and NaOH-silane-VF at 20% vetiver content.

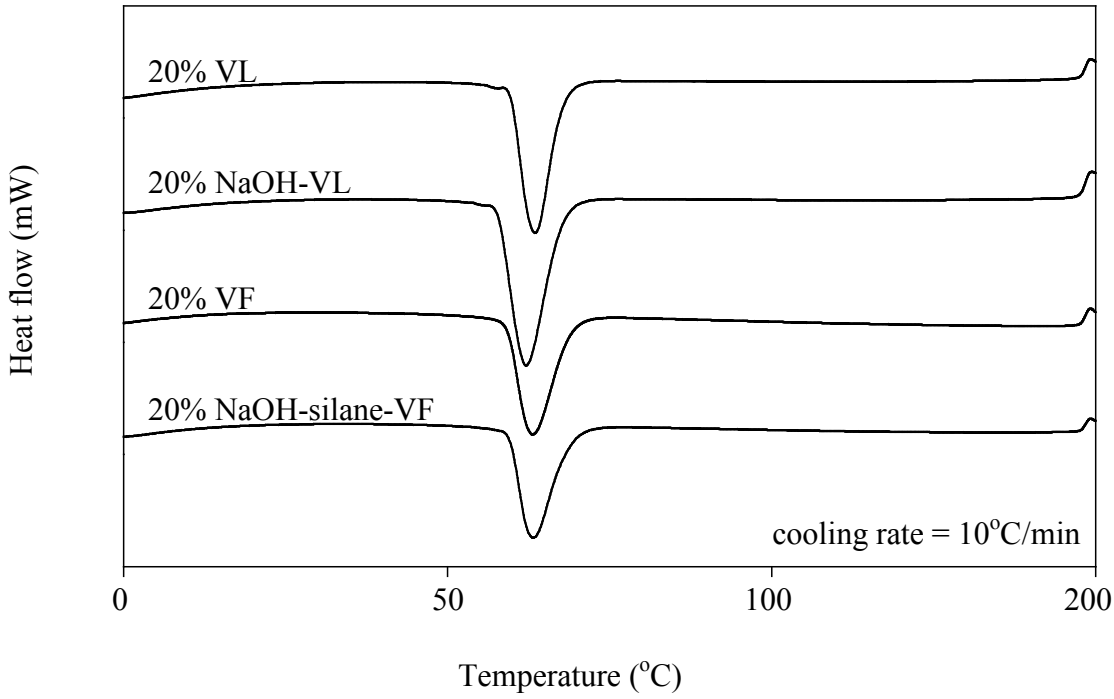

Figure 4.8 DSC curves corresponding to the cooling scans of vetiver-PP composites from VL, NaOH-VL, VF, and NaOH-silane-VF at 20% vetiver content.

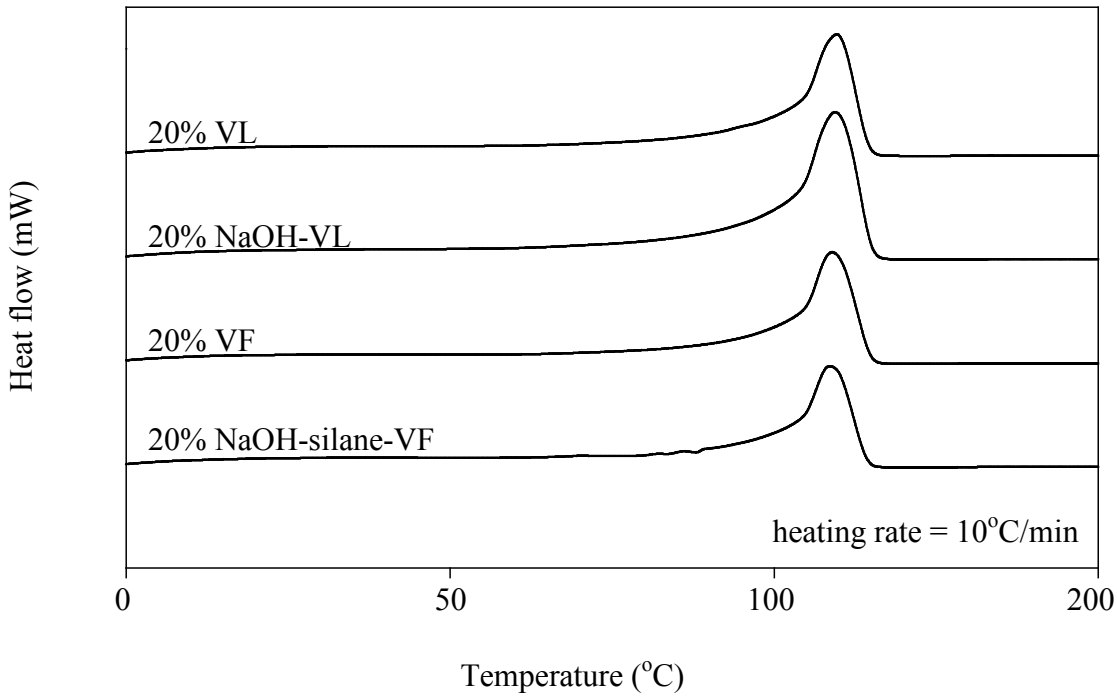

Figure 4.9 DSC curves corresponding to the second heating scans of vetiver-PP composites from VL, NaOH-VL, VF, and NaOH-silane-VF at 20% vetiver content.

The values of the melting temperature obtained from the second heating scans in Figure 4.9 are shown in Table 4.6. No significant change in melting temperature among the composites from VL, NaOH-VL, VF, and NaOH-silane-VF can be observed. The values of % crystallinity and crystallization temperature calculated from Figure 4.7 and Figure 4.8, respectively, are shown in Table 4.7. Crystallization temperature of the composites from VL, NaOH-VL, VF, and NaOH-silane-VF shows no significant difference. The % crystallinity of the composites from NaOH-VL is slightly higher than that of VL. This is because the NaOH can remove the impurities on the surface, which makes more nucleating sites for the

crystallization process. In addition, the % crystallinity of the composites from NaOH-silane-VF is slightly higher than that of VF. This may be due to the silane deposited on the fiber acting as nucleating agent for the crystallization process.

Table 4.6 Melting temperature of vetiver-PP composites from VL, NaOH-VL, VF, and NaOH-silane-VF at 20% vetiver content from the second heating scans.

Types of vetiver	**Melting temperature (^{o}C)**
VL	159
NaOH-VL	159
VF	159
NaOH-silane-VF	158

Table 4.7 Crystallization temperature and % crystallinity of vetiver-PP composites from VL, NaOH-VL, VF, and NaOH-silane-VF at 20% vetiver content.

Types of vetiver	**Crystallization temperature (^{o}C)**	**% Crystallinity (X_c)**
VL	113	36.1
NaOH-VL	112	38.7
VF	113	37.8
NaOH-silane-VF	113	40.6

4.3 Rheological properties of vetiver-PP composites

4.3.1 The effect of vetiver content on rheological properties of vetiver-PP composites

MFI of PP and vetiver-PP composites from VF at various vetiver contents are shown in Table 4.8. MFI of PP is higher than that of PP composites. With increasing vetiver content, the MFI of the composites decreases. This indicates that viscosity of the composites increases with increasing vetiver content. The decrease in the MFI of the composites is mainly influenced by the amount of the fiber in PP composites. A decrease in the MFI with increasing fiber content has also been found in the study of conifer-PP composites by Chuai et al. (2001).

Table 4.8 MFI of PP and vetiver-PP composites from VF at various vetiver contents.

Vetiver content (% wt)	**MFI (g/10min)**
0	3.02
5	2.83
10	2.09
20	1.17
30	0.65

Flow curves of PP composites from VL, NaOH-VL, and VF at various vetiver contents are shown in Figure 4.10-4.12, respectively. The vetiver-PP composites exhibit higher viscosity than that of PP. This is because the vetiver grass perturbs the normal flow of polymer and hinders the mobility of chain segments in melt flow. In addition, the viscosity of the vetiver-PP composites increases with increasing vetiver content. An increase in viscosity of the composites with increasing vetiver content is more predominant at low shear rate (10-10^2 s^{-1}) than that of at high shear rates (10^2-10^4 s^{-1}). This is similar to the results from the study of pineapple-LDPE composites, which have been reported that the viscosity of the composites increases with increasing fiber contents (George et al., 1996).

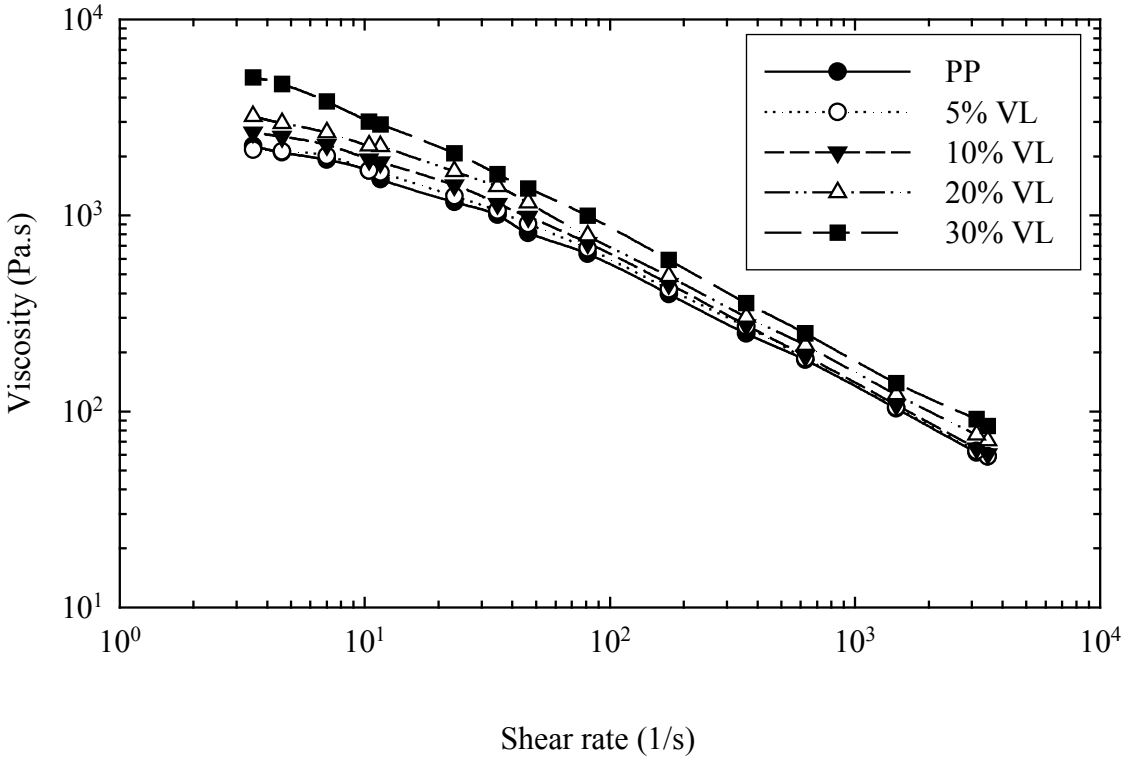

Figure 4.10 Flow curves of PP and vetiver-PP composites from VL at various vetiver contents.

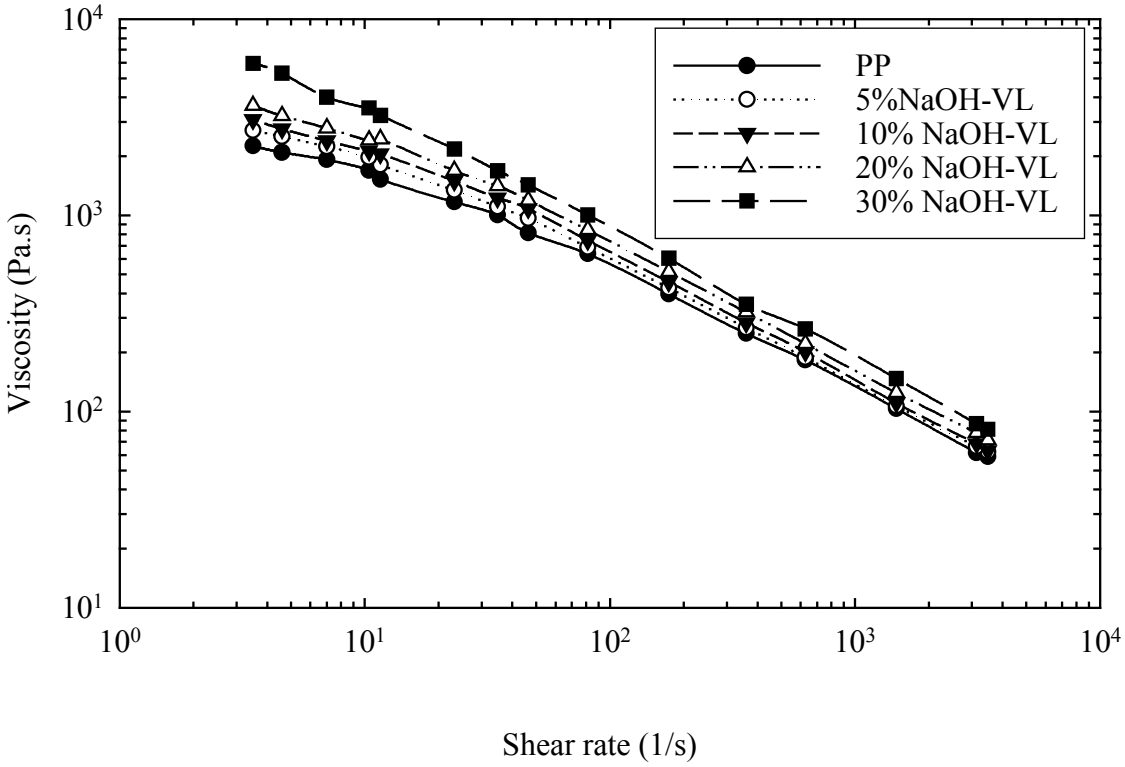

Figure 4.11 Flow curves of PP and vetiver-PP composites from NaOH-VL at various vetiver contents.

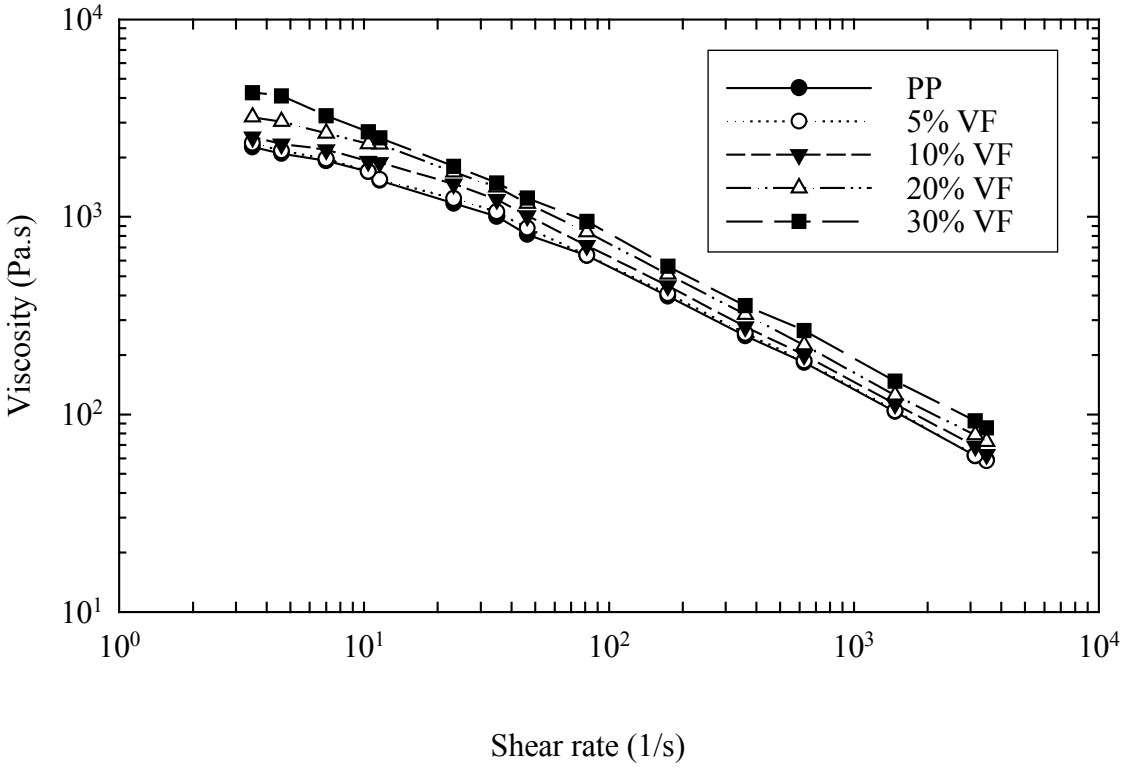

Figure 4.12 Flow curves of PP and vetiver-PP composites from VF at various vetiver contents.

4.3.2 The effect of chemical treatment on rheological properties of vetiver-PP composites

MFI of vetiver-PP composites from VL, NaOH-VL, VF, and NaOH-silane-VF at 20% vetiver content are shown in Table 4.9. The vetiver-PP composites from vetiver fiber (VF, NaOH-silane-VF) show slightly lower MFI than those of vetiver-PP composites from vetiver leaves (VL, NaOH-VL). This means that the viscosity of vetiver-PP composites from vetiver fiber is higher than those of vetiver leaves. This is also shown in the flow curves of vetiver-PP composites from VL, NaOH-VL, VF, and NaOH-silane-VF at 20% vetiver content in Figure 4.13. At high shear rate (10^2-10^4 s^{-1}), the viscosity of PP composites from VL, NaOH-VL, VF, and NaOH-silane-VF shows no difference.

Table 4.9 MFI of vetiver-PP composites from VL, NaOH-VL, VF, and NaOH-silane-VF at 20% vetiver content.

Types of vetiver	MFI (g/10min)
VL	1.66
NaOH-VL	1.36
VF	1.17
NaOH-silane-VF	1.17

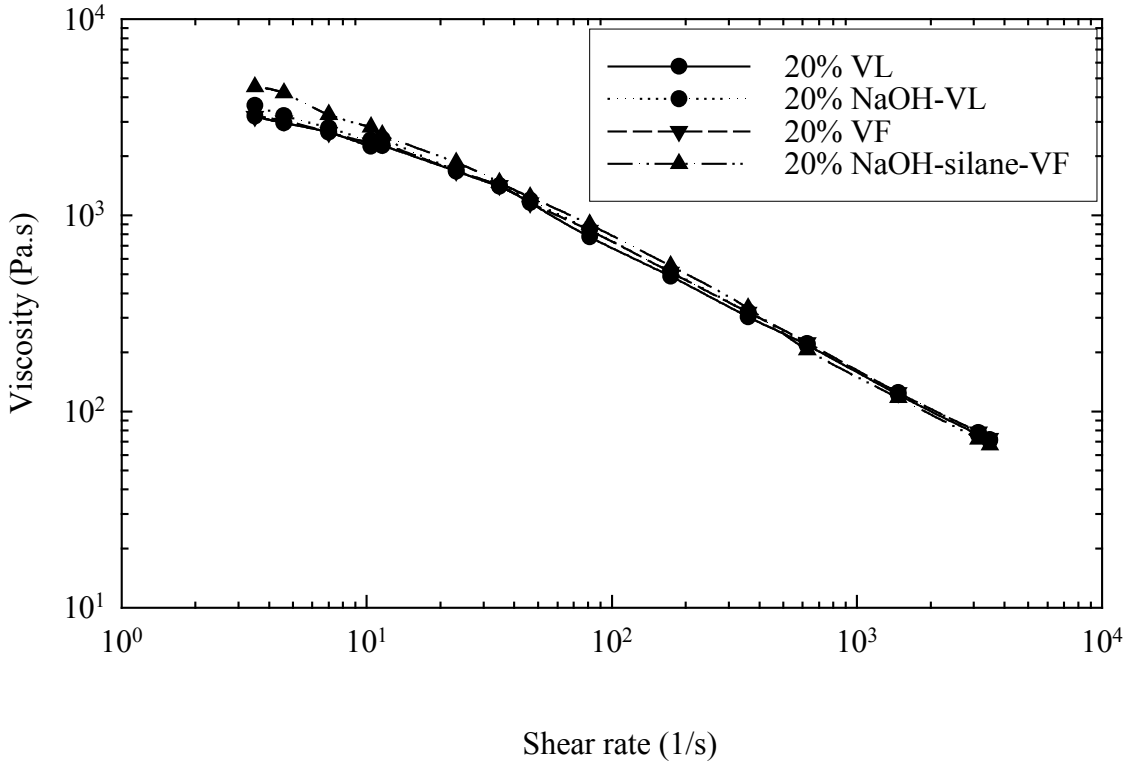

Figure 4.13 Flow curves of vetiver-PP composites from VL, NaOH-VL, VF, and NaOH-silane-VF at 20 % vetiver content.

4.4 Mechanical properties of vetiver-PP composites

4.4.1 The effect of vetiver length on mechanical properties of vetiver-PP composites

The effect of vetiver length on tensile strength, Young's modulus, elongation at break, and impact strength of vetiver-PP composites from NaOH-VL at 20% vetiver content are shown in Table 4.10 and Figure 4.14-4.15. The vetiver-PP composites at various vetiver lengths show no differences in tensile strength and Young's modulus. Elongation at break of the composites slightly decreases at vetiver length of 4 mm. With increasing vetiver length, a slight decrease in impact strength of the composites can be observed. During the processing of the composites, some vetiver grass at longer vetiver lengths may be broken into shorter length. The final length of NaOH-VL in the composites prepared from various vetiver lengths may not be much different. This may cause no significant change in mechanical properties of the composites. Similarly, a study of flax-PP composite (Garkhail et al., 2000) and sisal-PP composite (Joseph et al., 1999) have shown that tensile strength of the composites does not change when fiber length is longer than 5 mm.

Table 4.10 Tensile strength, Young's modulus, elongation at break, and impact strength of vetiver-PP composites from NaOH-VL at 20% vetiver content.

Vetiver lengths (mm)	Tensile strength (MPa)	Young's modulus (MPa)	Elongation at break (%)	Impact strength (kJ/m^2)
0.10	24.93 ± 0.86	592.45 ± 36.19	11.30 ± 0.54	20.32 ± 1.15
2.00	26.08 ± 0.69	548.18 ± 49.17	11.33 ± 0.77	18.97 ± 1.51
4.00	25.92 ± 0.40	573.30 ± 27.65	9.19 ± 0.33	15.62 ± 2.19

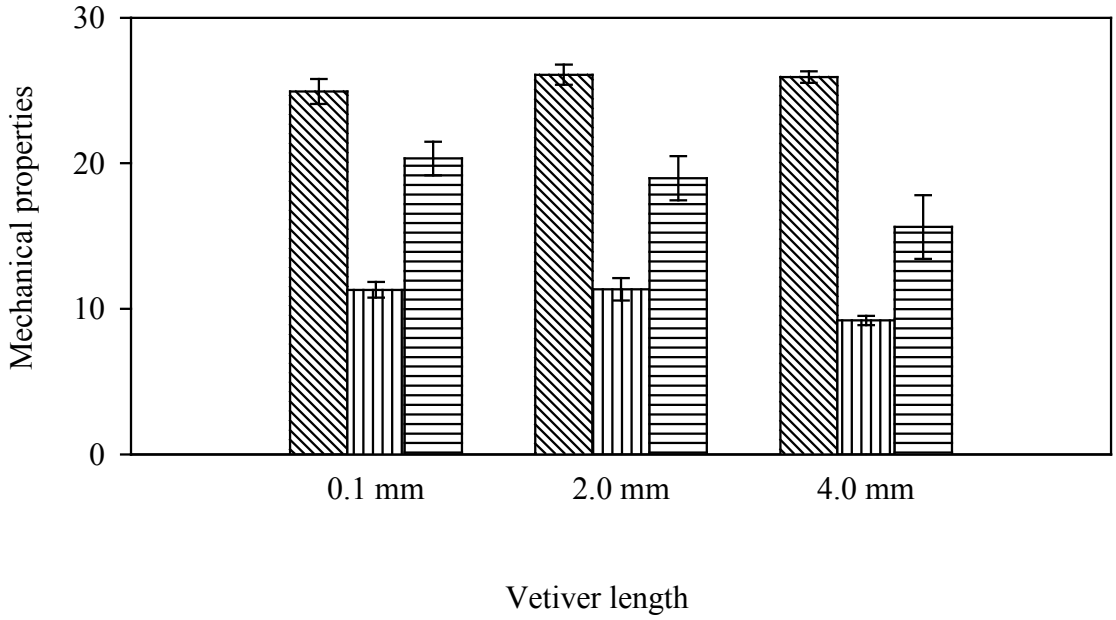

Figure 4.14 Tensile strength (MPa) (▨), elongation at break (%) (▥), and impact strength (kJ/m^2) (▤) of vetiver-PP composites from NaOH-VL at 20% vetiver content.

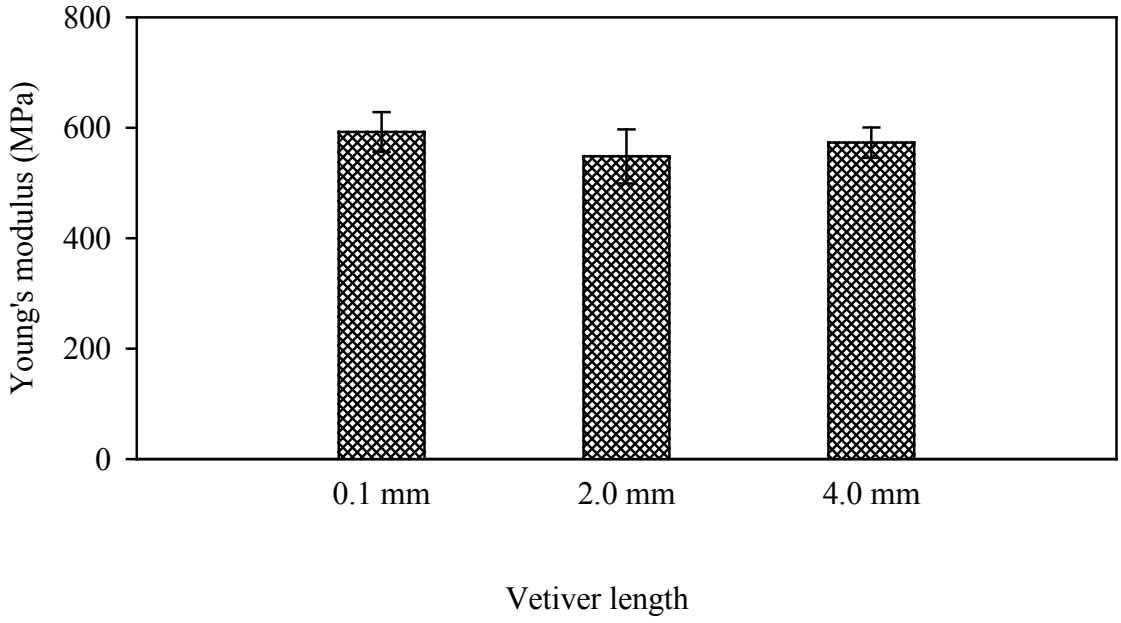

Figure 4.15 Young's modulus of vetiver-PP composites from NaOH-VL at 20% vetiver content.

4.4.2 The effect of mixing procedures on mechanical properties of vetiver-PP composites

The tensile strength, Young's modulus, elongation at break, and impact strength of 20% vetiver-PP composites from NaOH-VL at vetiver length of 2 mm by different mixing procedures, method A and B according to section 3.2.2 are shown in Table 4.11. The differences of the two methods are the sequence of adding NaOH-VL in the composites and the mixing time after adding NaOH-VL. In method A, NaOH-VL was added after melting PP for 5 min and the mixing time after adding NaOH-VL was 5 min. In method B, NaOH-VL and PP were mixed together for 10 min. The tensile strength and impact strength of the composites from method A and method B show no significant differences. Nevertheless, Young's modulus of the composites

from method B is higher than that of the composites from method A. However, the elongation at break from method B is lower than that of the composites from method A. This can be explained as follow; the longer mixing time of NaOH-VL in the composites leads to the better dispersion of vetiver in PP matrix. On the other hands, the longer mixing time may cause the degradation of the vetiver due to the low thermal resistance of the vetiver.

Table 4.11 Tensile strength, Young's modulus, elongation at break, and impact strength of 20% vetiver-PP composites from NaOH-VL with vetiver length of 2 mm by different mixing procedures.

Methods	Tensile strength (MPa)	Young's modulus (MPa)	Elongation at break (%)	Impact strength (kJ/m^2)
A	26.08 ± 0.69	548.18 ± 49.17	11.33 ± 0.77	18.97 ± 1.51
B	25.73 ± 0.26	1220.00 ± 50.35	7.90 ± 0.70	17.25 ± 0.95

4.4.3 The effect of vetiver content on mechanical properties of vetiver-PP composites

The effect of vetiver content on tensile strength, Young's modulus, elongation at break, and impact strength of vetiver-PP composites from NaOH-VL at various vetiver contents are given in Table 4.12 and Figure 4.16-4.17. The tensile strength of vetiver-PP composites slightly decreases with increasing vetiver content. This may be because the increasing vetiver content facilitates a slipping of fiber and PP matrix. Also, the reduction of the tensile strength at higher vetiver content is

attributed to an increase in number of void in the composites, which is served as a local area for crack initiation and causes the failure at lower stress. A decrease in tensile strength with increasing fiber content has also been observed in the PP composites from kudzu, conifer, and sisal fiber (Luo et al., 2002; Chuai et al., 2001; Fung et al., 2002; Liau et al., 1997). In contrast, the study of sisal-PP composites has shown an increase in tensile strength with increasing fiber content (Joseph et al., 1995). However, no significant change in tensile strength with increasing fiber content has been found in the study of kenaf-PP composite (Karnani et al., 1999).

From Figure 4.16, elongation at break of vetiver-PP composites decreases with increasing vetiver content. This is because vetiver grass has lower elongation at break than that of PP. A decrease in elongation at break with increasing fiber content was also observed in the study of conifer-PP composites and wood-PP composites (Chuai et al., 2000; Coutinho et al., 1997). In addition, Liau et al. (1997) have found that elongation at break decreases drastically with increasing wood content in LDPE composites.

The impact strength of PP can not be obtained because it does not break within the limit of an instrument (maximum energy of 5.4 J). However, this implies that the impact strength of vetiver-PP composites is lower than that of PP. The impact strength of the composites decreases with increasing vetiver content. The higher amount of NaOH-VL also increases a probability of NaOH-VL agglomeration and creates void in the composites. This leads to poor adhesion between vetiver and PP matrix and causes more crack initiation, which leads to the composites failure. As a result, the impact strength decreases with increasing vetiver content. This is similar to the studies of the kenaf-PP composite studied by Karnani et al. (1997) and Sanadi

et al. (1995). They have found that the impact strength of composites slightly decreases with increasing kenaf content.

Table 4.12 Tensile strength, Young's modulus, elongation at break, and impact strength of vetiver-PP composites from NaOH-VL at various vetiver contents.

Vetiver content (% wt)	**Tensile strength (MPa)**	**Young's modulus (MPa)**	**Elongation at break (%)**	**Impact strength (kJ/m^2)**
0	12.58 ± 0.45*	732.45 ± 14.13*	94.25 ± 0.70*	>119.60
5	27.08 ± 0.26	809.52 ± 42.48	16.63 ± 1.02	30.66 ± 3.34
10	26.60 ± 0.59	925.83 ± 47.36	12.44 ± 0.93	21.43 ± 1.12
20	25.73 ± 0.26	1220.00 ± 50.35	7.90 ± 0.70	17.25 ± 0.95
30	25.12 ± 0.59	1565.00 ± 44.22	6.12 ± 0.47	16.65 ± 1.09

* Test speed 50 mm/min

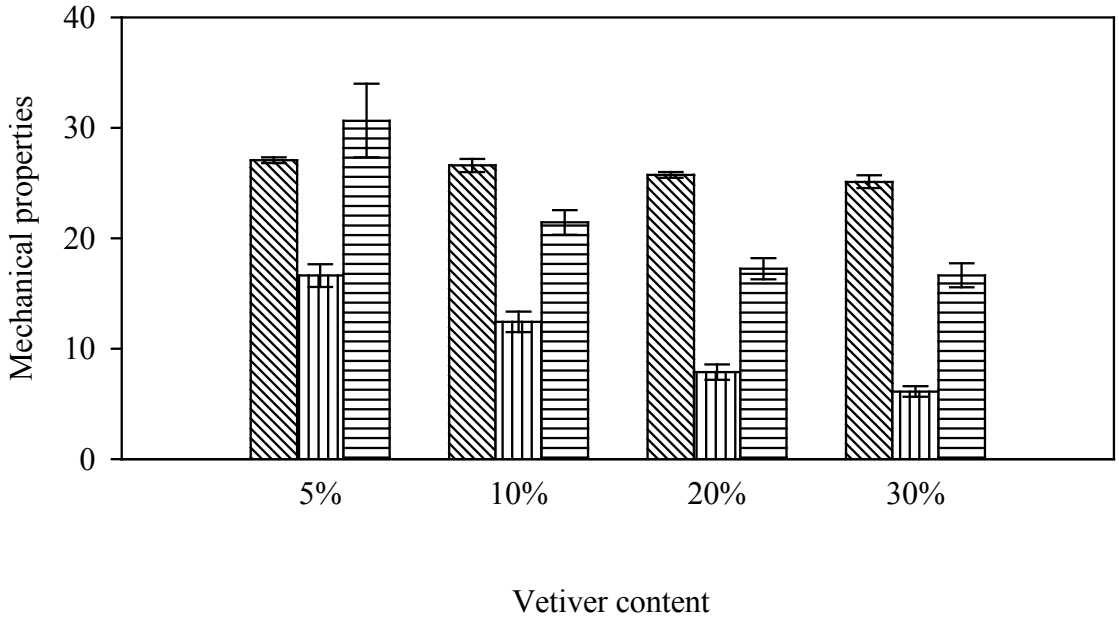

Figure 4.16 Tensile strength (MPa) (▨), elongation at break (%) (▥), and impact strength (kJ/m^2) (▤) of vetiver-PP composites from NaOH-VL at various vetiver contents.

From Figure 4.17, the Young's modulus of vetiver-PP composites increases with increasing vetiver content. This is because the Young's modulus of vetiver grass according to Table 4.1 (23.2 GPa) is much higher than that of PP (0.8 GPa). This results in the increase of Young's modulus of the composites. An increase in Young's modulus of the composites with increasing fiber content has also been observed in PP composites from sisal, kenaf, coir, hemp, jute, and wood fiber (Joseph et al., 1999; Luo et al., 2002; Wambua et al., 2003; Coutinho et al., 1997; Liau et al., 1997).

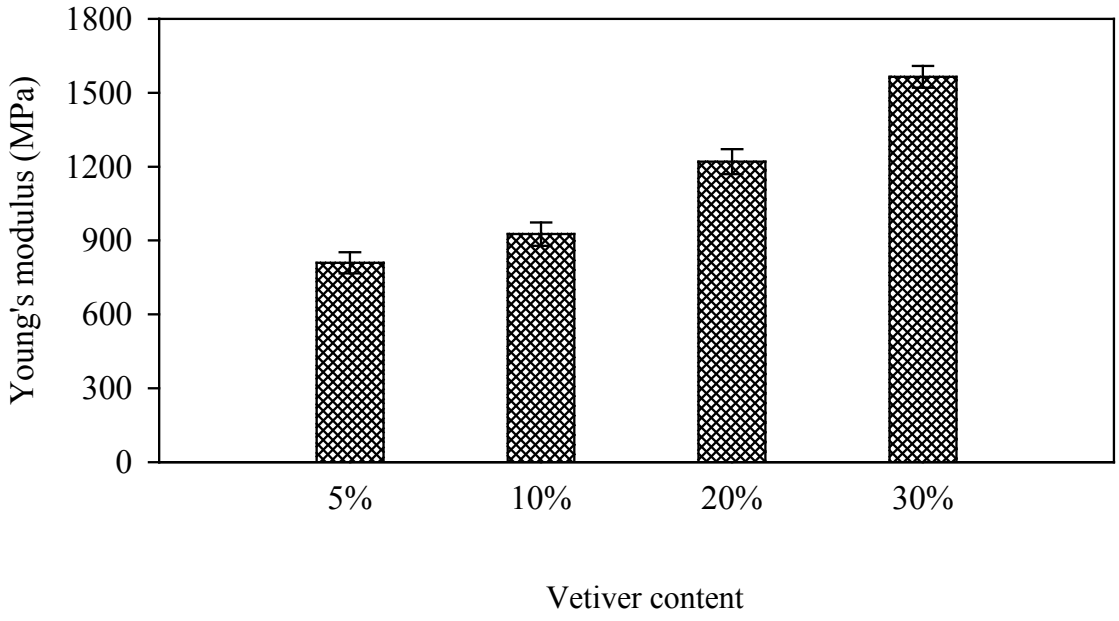

Figure 4.17 Young's modulus of vetiver-PP composites from NaOH-VL at various vetiver contents.

HDT of PP and vetiver-PP composites from VF at various vetiver contents are shown in Table 4.13. The HDT of vetiver-PP composites increases with increasing vetiver contents. At vetiver content of 30%, the HDT of the composites increases up to 64% compared to that of PP. From the study of conifer-PP composites, the HDT of the composites increases about 2% compared to that of PP (Chuai et al., 2001).

Table 4.13 HDT of PP and vetiver-PP composites from VF at various vetiver contents.

Vetiver content (% wt)	**HDT (^{o}C)**
0	81 ±1.0
5	94 ± 0.5
10	109 ± 1.0
20	125 ± 0.0
30	133 ± 1.0

4.4.4 The effect of chemical treatment on mechanical properties of vetiver-PP composites

The tensile strength, Young's modulus, elongation at break, and impact strength of vetiver-PP composites from VL, NaOH-VL, VF, and NaOH-silane-VF are given in Table 4.14 and Figure 4.18-4.19. The tensile strength, Young's modulus, elongation at break, and impact strength of vetiver-PP composites from NaOH-VL are slightly higher than that of vetiver-PP composites from VL. In addition, tensile strength, Young's modulus, elongation at break, and impact strength of vetiver-PP composites from NaOH-silane-VF are slightly higher than that of PP composites from VF. This may be due to the physical bonding or chemical bonding between NaOH-silane-VF and PP matrix. The reason why NaOH treatment improves the mechanical properties of the composites will be discussed along with the morphological properties in section 4.5. Similarly, several authors have reported that the silane treatment improves the mechanical properties of kenaf-PP composites and sisal-PP composite (Joseph et al., 1999; Karnani et al., 1997; Valadez et al., 1999).

Table 4.14 Tensile strength, Young's modulus, elongation at break, and impact strength of vetiver PP composites from VL, NaOH-VL, VF, and NaOH-silane-VF at 20% vetiver content.

Types of vetiver	Tensile strength (MPa)	Young's modulus (MPa)	Elongation at break (%)	Impact strength (kJ/m^2)
VL	25.14 ± 0.41	1196.98 ± 41.13	7.27 ± 0.67	15.79 ± 0.32
NaOH-VL	25.73 ± 0.26	1220.00 ± 50.35	7.90 ± 0.70	17.25 ± 0.95
VF	24.32 ± 0.46	954.33 ± 38.13	8.17 ± 0.40	17.14 ± 0.83
NaOH-silane-VF	24.53 ± 0.14	1051.93 ± 29.34	9.30 ± 0.70	20.44 ± 0.53

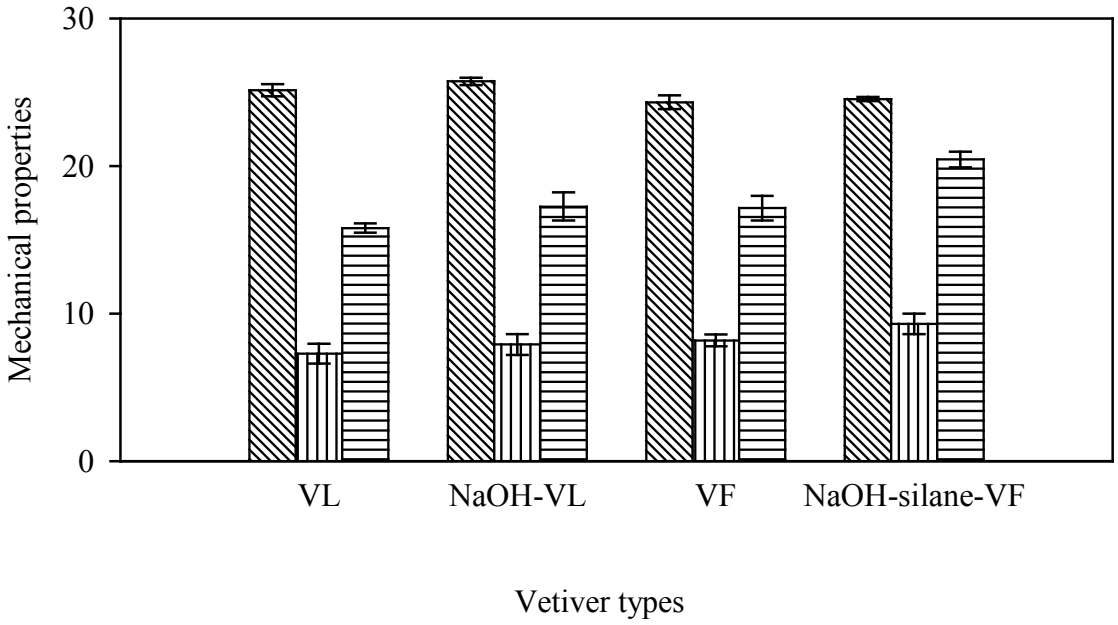

Figure 4.18 Tensile strength (MPa) (▨), elongation at break (%) (▥), and impact strength (kJ/m^2) (▤) of vetiver-PP composites from VL, NaOH-VL, VF, and NaOH-silane-VF at 20% vetiver content.

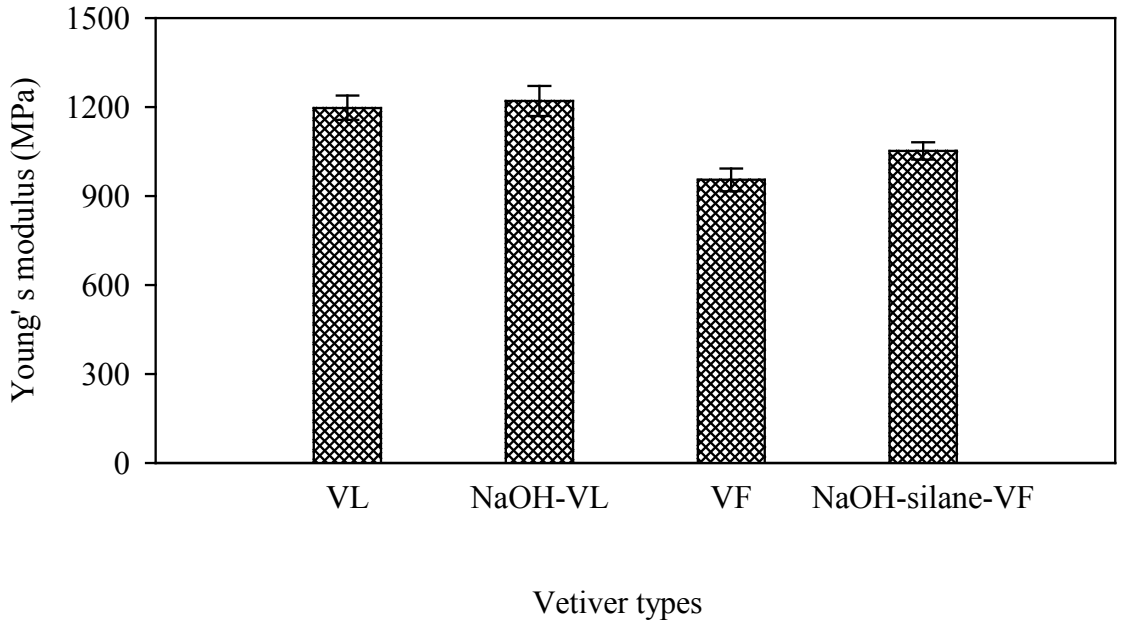

Figure 4.19 Young's modulus of vetiver-PP composites from VL, NaOH-VL, VF, and NaOH-silane-VF at 20% vetiver content.

HDT of vetiver-PP composites from VL, NaOH-VL, VF, and NaOH-silane-VF at 20% vetiver content are shown in Table 4.15. It shows no significant difference in HDT of vetiver-PP composites from VL, NaOH-VL, VF, and NaOH-silane-VF.

Table 4.15 HDT of vetiver-PP composites from VL, NaOH-VL, VF, and NaOH-silane-VF at 20% vetiver content.

Types of vetiver	**HDT (^{o}C)**
VL	123 ± 0.6
NaOH-VL	124 ± 0.6
VF	125 ± 0.0
NaOH-silane-VF	125 ± 0.6

4.5 Morphological properties of vetiver grass and vetiver-PP composites

4.5.1 The effect of chemical treatment on morphological properties of vetiver grass

The SEM micrographs of VL, NaOH-VL, VF, and NaOH-silane-VF, are shown in Figure 4.20a-4.20d, respectively. These micrographs reveal the effect of NaOH treatment on the microstructure of NaOH-VL and NaOH-silane-VF. The treatment results in the removal of some impurities. In addition, NaOH treatment breaks down the composite fiber bundle into smaller fibers. These increase the effective surface area available for contact between NaOH-VL and PP matrix. Also in the case of NaOH-silane-VF, the NaOH treatment improves the deposition of silane onto the fibers. This may cause more physical or chemical bonding between NaOH-silane-VF and PP matrix. Therefore, the NaOH treatment results in the better mechanical properties of the composites from NaOH-VL and NaOH-silane-VF. Similarly, many researchers have reported that NaOH treatment on jute, sisal, hemp, and oil palm fibers can partially remove the hemicellulose, waxes and lignin present on the surface of fiber. (Sydenstricker et al., 2003; Razerra and Frollini, 2004; Lu et al., 2003; Mishra et al., 2001; George et al., 2001; Iannace et al., 2001; Mwaikambo and Ansell, 1999).

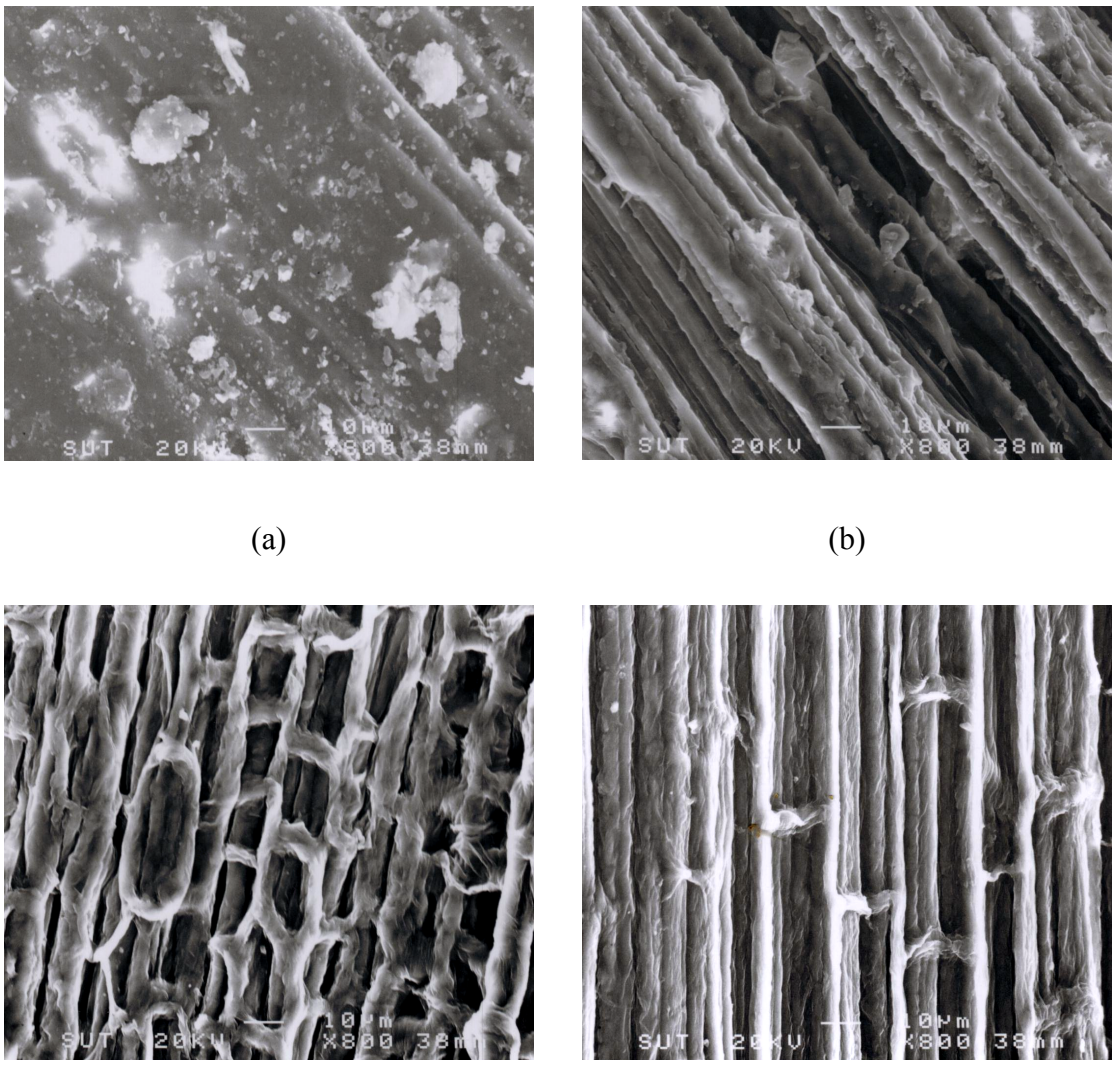

(a) (b)

(c) (d)

Figure 4.20 SEM micrographs of vetiver grass: (a) VL, (b) NaOH-VL, (c) VF, and (d) NaOH-silane-VF.

4.5.2 The effect of time of treatment on morphological properties of vetiver grass

The SEM micrographs of untreated VF and treated VF with 5% NaOH solution by various time of treatment are shown in Figure 4.21. NaOH treated VF are cleaner and fiber bundle are more separated compared with the untreated fiber. With increasing time of treatment from 2 to 4 hours, SEM micrographs of NaOH treated VF shows that fiber bundles are better separated into smaller fiber. SEM micrograph of NaOH treated VF at 6 hours show no significant difference from NaOH treated VF at 4 hours. In addition, Ray and Sarkar (2001) have studied the effect of NaOH treatment on morphology of jute fiber by treating jute fiber with 5% concentration of NaOH solution for 2, 4, 6, and 8 hours. They have reported that the hemicellulose content of the jute fibers reduces with increasing NaOH treatment time. The large loss of hemicellulose made the fibers loss their cementing capacity. Then the jute fiber can separate out from each other.

4.5.3 The effect of vetiver content on morphological properties of vetiver-PP composites

SEM micrographs of fracture surfaces of PP composites from VF at different vetiver contents are shown in Figure 4.22. With increasing vetiver contents, SEM micrographs show more agglomeration of vetiver fiber. This results in lower tensile strength and impact strength of the composites.

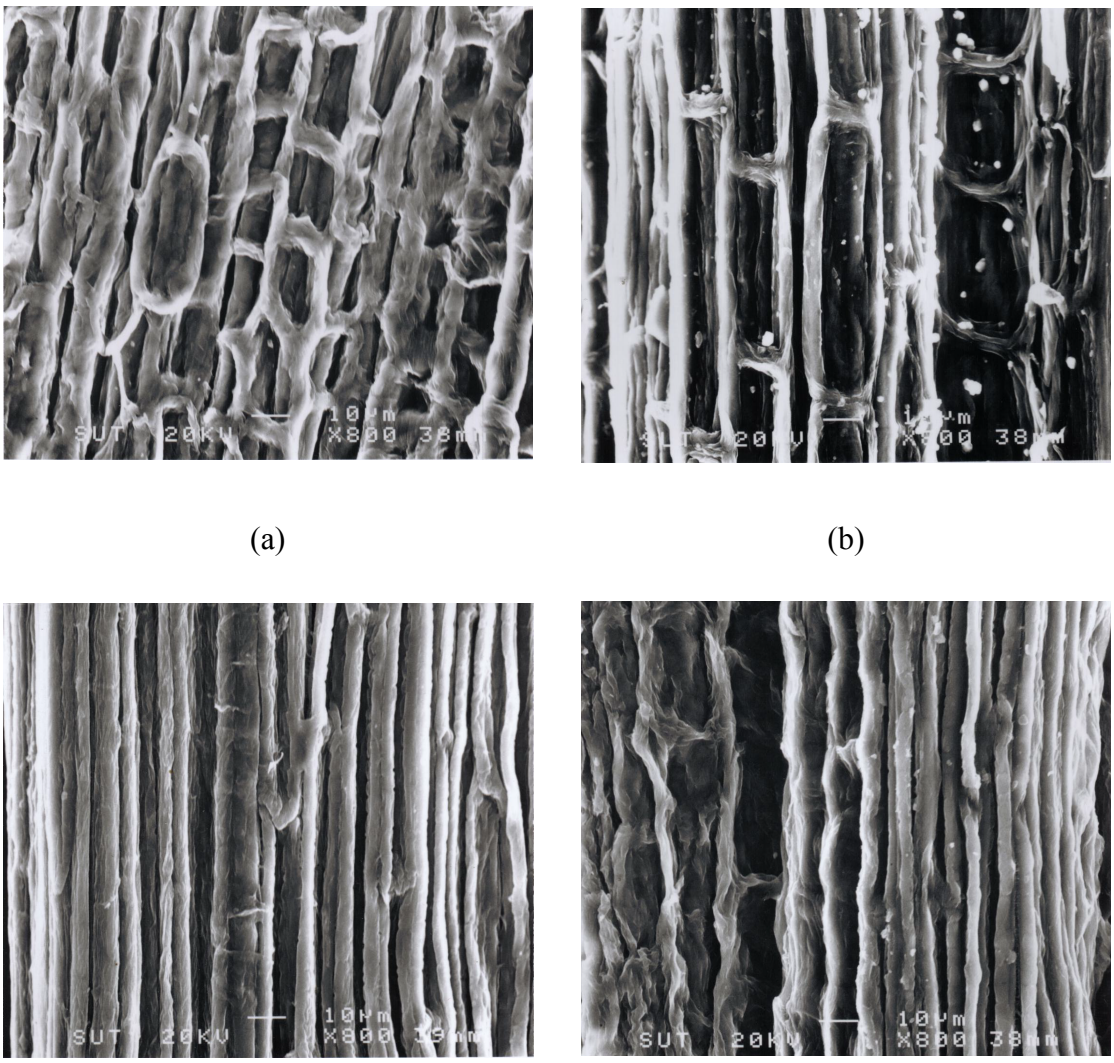

(a) (b)

(c) (d)

Figure 4.21 SEM micrographs of NaOH treated VF at various time of treatment (a) 0 h, (b) 2 h, (c) 4 h, and (d) 6 h.

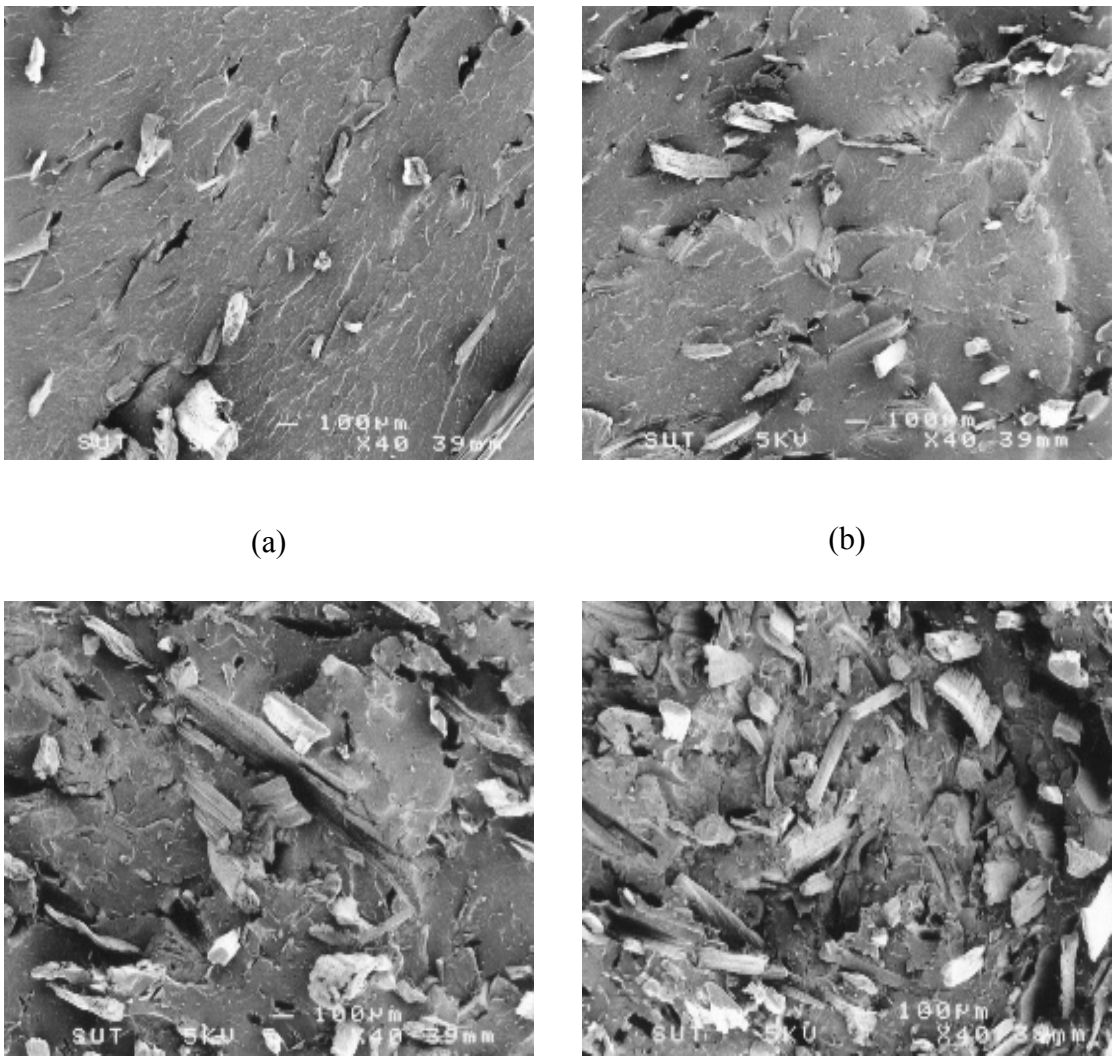

(a) (b)

(c) (d)

Figure 4.22 SEM micrographs of fracture surfaces of vetiver-PP composites from VF at various vetiver contents (a) 5%, (b) 10%, (c) 20%, and (d) 30%.

4.6 Shear-induced crystallization of vetiver-PP composites

4.6.1 The effect of vetiver content on shear-induced crystallization of vetiver-PP composites

The optical micrographs of PP and VF-PP composites at various vetiver contents from the injection molded samples are shown in Figure 4.23a-4.23e, respectively. All composites comprise of two layers, skin and core, which show an alignment of VF along the flow direction in composites. The skin layer or shear-induced crystallization layer is a highly oriented flow-induced microstructure, which is frozen in by the crystallization process (Karger-Kocsis, 1995; Wang et al., 2004). The value of normalized thickness of skin layer of PP and vetiver-PP composites at various vetiver contents obtained from Figure 4.23 are given in Table 4.16. With increasing vetiver contents, normalized thickness of skin layer does not significantly change. This indicates that fibers in composites do not affect shear-induced crystallization. It implies that the change in mechanical properties of the composites with increasing vetiver content is not caused by shear-induced crystallization.

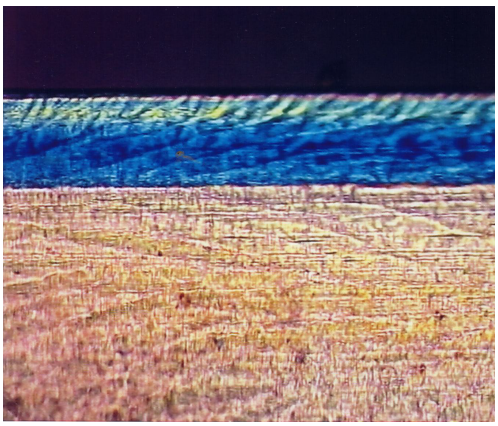

(a)

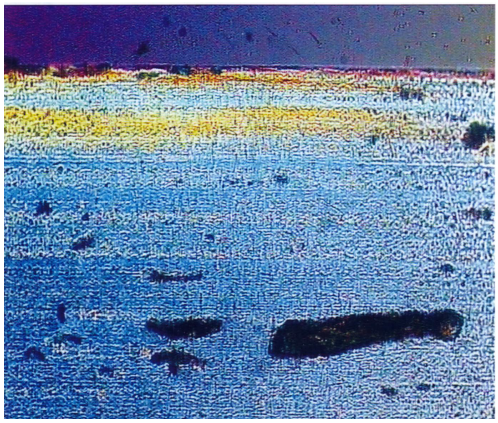

(b)

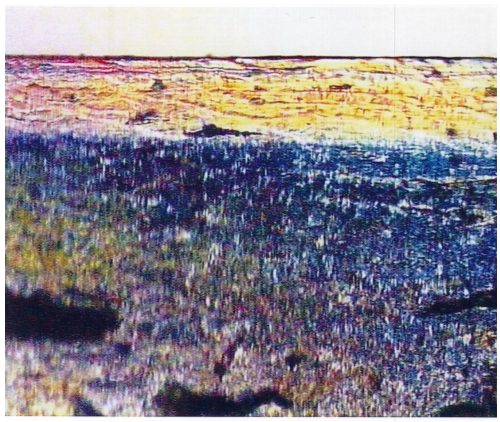

(c)

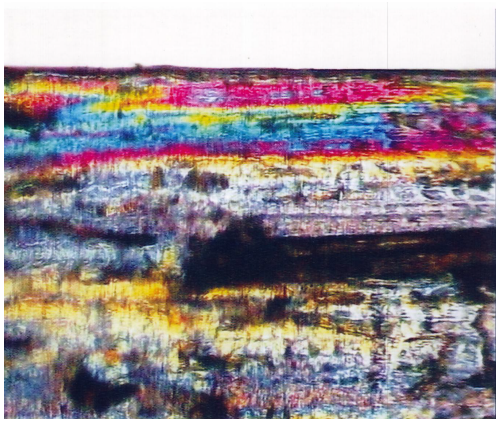

(d)

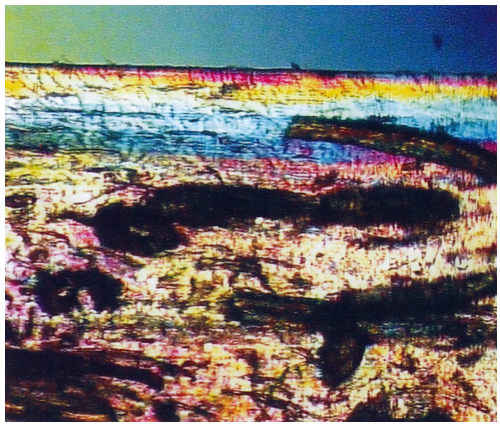

(e)

Figure 4.23 Optical micrographs of vetiver-PP composites from VF at various vetiver contents (a) 0%, (b) 5%, (c) 10%, (d) 20%, and (e) 30%.

Table 4.16 Normalized thickness of skin layer of PP and vetiver-PP composites from VF at various vetiver contents.

Vetiver content (% wt)	Normalized thickness of skin layer (%)
0	9.89
5	7.22
10	8.89
20	9.44
30	10.03

4.6.2 The effect of chemical treatment on shear-induced crystallization of vetiver-PP composites

The optical micrographs of vetiver-PP composite at 20% vetiver content from different forms of vetiver, i.e., VL, NaOH-VL, VF, and NaOH-silane-VF are shown in Figure 4.24a-4.24d, respectively. The value of normalized thickness of skin layer of vetiver-PP composites from VL, NaOH-VL, VF, and NaOH-silane-VF at 20% vetiver content obtained from Figure 4.24 are given in Table 4.17. The vetiver-PP composites from VL, NaOH-VL, VF, and NaOH-silane-VF show no difference in normalized thickness of skin layer.

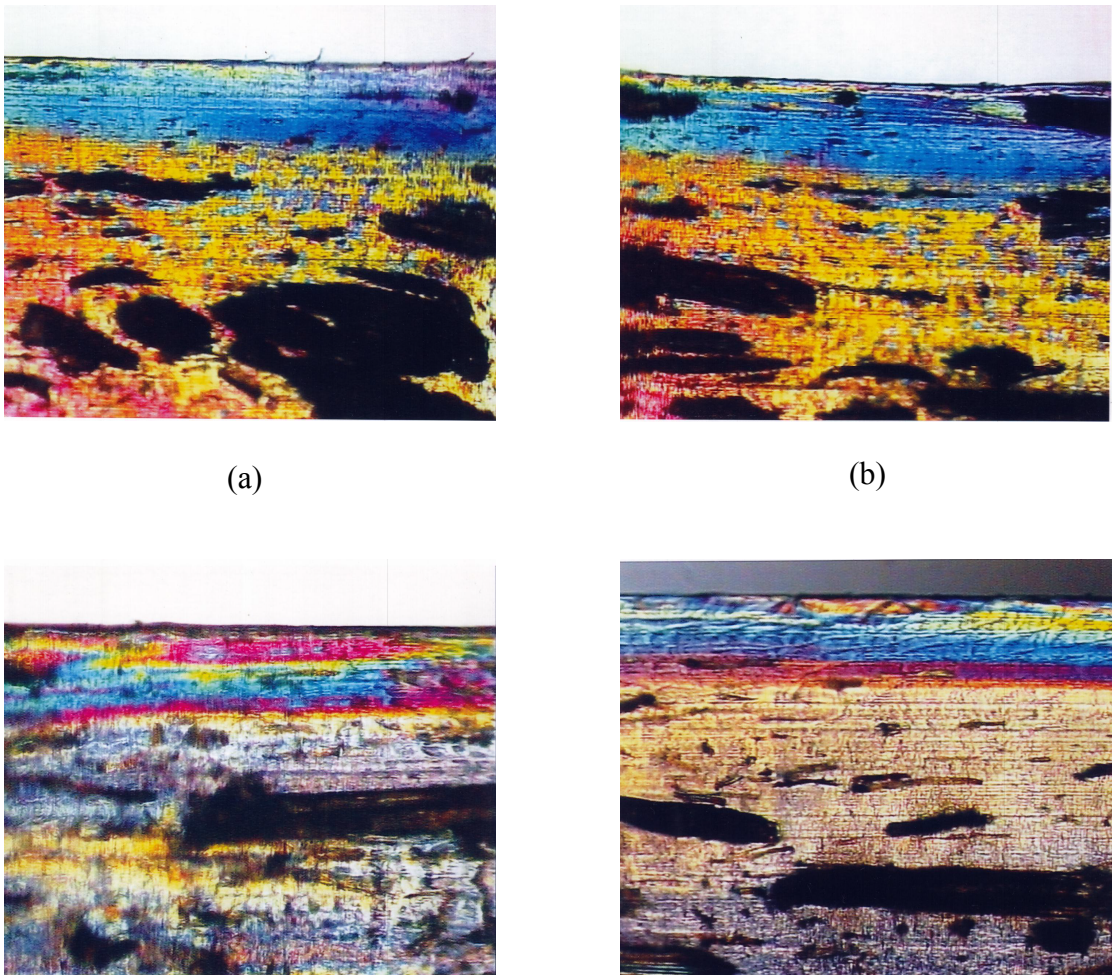

(a) (b)

(c) (d)

Figure 4.24 Optical micrographs of vetiver-PP composites at 20% vetiver content from different forms of vetiver (a) VL, (b) NaOH-VL, (c) VF, and (d) NaOH-silane-VF.

Table 4.17 Normalized thickness of skin layer of vetiver-PP composites from VL, NaOH-VL, VF, and NaOH-silane-VF at 20% vetiver content.

Types of vetiver	**Normalized thickness of skin layer (%)**
VL	8.91
NaOH-VL	9.44
VF	9.44
NaOH-silane-VF	9.47

CHAPTER V

CONCLUSIONS

The effects of chemical treatment and vetiver content on thermal properties of vetiver grass and vetiver-PP composites were elucidated in this study. There was no significant difference in hemicellulose decomposition temperature of VL, NaOH-VL, VF, and NaOH-silane-VF (310^{o}C-312^{o}C). In addition, the decomposition temperatures of α-cellulose of NaOH-VL, VF, and NaOH-silane-VF were in the same range (343^{o}C-348^{o}C). In case of VL, the decomposition temperature of -cellulose can not be observed as a peak in DTG curves. However, the beginning of decomposition temperature can be observed around 333^{o}C from DTG curves. The decomposition temperature of vetiver-PP composites decreased with increasing vetiver content due to the low thermal stability of vetiver grass. In addition, the decomposition temperature of α-cellulose of the composites was higher than that of vetiver grass. The vetiver-PP composites with increasing vetiver contents showed no significant change in melting temperature. The crystallization temperature of vetiver-PP composites increased with increasing vetiver contents. The % crystallinity of vetiver-PP composites decreased with increasing vetiver contents. The melting temperature of the vetiver-PP composite from VL, NaOH-VL, VF, and NaOH-silane-VF showed no significant difference. The crystallization temperature of vetiver-PP composite from VL, NaOH-VL, VF, and NaOH-silane-VF showed no difference. The % crystallinity of vetiver-PP composites from NaOH-VL was slightly higher than that

of VL. In addition, % crystallinity of vetiver-PP composites from NaOH-silane-VF was slightly higher than that of VF.

The effects of vetiver content and chemical treatment on rheological properties of vetiver-PP composites were studied. The viscosity of vetiver-PP composites increased with increasing vetiver contents. The chemical treatment showed no effect on the viscosity of vetiver-PP composites.

The effects of vetiver length, mixing procedure, vetiver content, and chemical treatment on mechanical properties of vetiver-PP composites were shown in this study. The vetiver-PP composites at various vetiver lengths showed no significant change in mechanical properties of the composites. The tensile strength and impact strength of the composites from method A and method B showed no significant differences. Nevertheless, Young's modulus of the composites from method B was higher than that of the composites from method A while the elongation at break from method B was lower than that of the composites from method A. Compared to PP, vetiver-PP composites showed higher tensile strength and Young's modulus but lower elongation at break and impact strength. With increasing vetiver contents, tensile strength, elongation at break, and impact strength of vetiver-PP composites slightly decreased while Young's modulus increased. Moreover, HDT of vetiver-PP composites increased with increasing vetiver content. In addition, the chemical treatment can improve the mechanical properties of the composites.

The effects of chemical treatment and vetiver content on morphological properties of vetiver grass and vetiver-PP composite were investigated. The NaOH treatment broke down the vetiver bundle into smaller fibers. These increased the effective surface area available for contact between fiber and matrix, which resulted in the

better mechanical properties of the composites. SEM micrographs of fracture surfaces of PP composites from VF showed more agglomeration of vetiver fiber with increasing vetiver contents.

The vetiver content and chemical treatment showed no effect on shear-induced crystallization of vetiver-PP composites.

REFERENCES

Albano, C., Gonzalez, J., Ichazo, M., and Kaiser, D. (1999). Thermal stability of blend of polyolefins and sisal fiber. **Polym. Degrad. Stability.** 66: 179-190.

Amash, A., and Zugenmaier, P. (2000). Morphology and properties of isotropic and oriented samples of cellulose fibre-polypropylene composites. **Polymer.** 41: 1589-1596.

Bledzki, A. K., and Gassan, J. (1999). Composites reinforced with cellulose based fibres. **Prog. Polym. Sci.** 24: 221-274.

Bisanda, E. T. N. (2000). The effect of Alkali treatment on the adhesion characteristic of sisal fibers. **Appl. Comp. Mater.** 7: 331-339.

Bruijn, J. C. M. (2000). Natural fibre mat thermoplastic products from a processor's point of view. **Appl. Comp. Mater.** 7: 415-420.

Cantero, G., Arbelaiz, A., Llano-Ponte, R., and Mondragon, I. (2003). Effect of fibre treatment on wettability and mechanical behavior of flax/polypropylene composites **Comp . Sci. Technol.** 63: 1247-1254.

Chuai, C., Almdal, K., Poulsen, L., and Plackett, D. (2000). Conifer fibers as reinforcing materials for polypropylene-based composites**. J. Appl. Polym. Sci.** 80: 2833-2841.

Cook, G. J. (1993). **Handbook of textile fibres.** England: Merrow.

Coutinho, F. M. B., Costa, T. H. S., and Carvalho, D. L. (1997). Polypropylene-wood fiber composites: effect of treatment and mixing conditions on mechanical properties. **J. Appl. Polym. Sci.** 65: 1227-1235.

Devi, L. U., Bhagawan, S. S., and Thomas, S. (1997). Mechanical properties of pineapple leaf fiber reinforced polyester composites. **J. Appl. Polym. Sci.** 64: 1739-1748.

Eichhon, S. J., et al. (2001). Review current international research into cellulose fibres and composites. **J. Mater. Sci.** 36: 2107-2131.

Fung, K. L., Li, R. K. Y., and Tjong, S. C. (2002). Interface modification on the properties of sisal fiber-reinforced polypropylene composites. **J. Appl. Polym. Sci.** 85: 169-176.

Garkhail, S. K., HeijenRath, R. W. H, and Peijs, T. (2000). Mechanical properties of natural-fiber-mat reinforced thermoplastics based on flax fibers and polypropylene. **Appl. Comp. Mater.** 7: 351-372.

Gassan, J. and Bledzki, A. K. (1997). The influence of fiber-surface treatment on the mechanical properties of jute-polypropylene composites. **Comp. Part A.** 28A: 1001-1005.

Gassan, J. and Bledzki, A. K. (1999). Possibilities for improving the mechanical properties of jute/epoxy composites by alkali treatment of fibres. **Comp. Sci. Technol.** 59 :1303-1309.

Gassan, J. and Bledzki, A. K. (1997). **Polym. Comp.** 18: 179-184. Quoted in Bledzki, A. K. and Gassan, J. (1999). Composites reinforced with cellulose based fibres. **Prog. Polym. Sci.** 24: 221-274.

George, J., Bhagawan, S. S., and Thomas, S. (1998). Effect of environment on the properties of low density polyethylene composites reinforced with pineapple leaf fiber. **Comp. Sci. Technol.** 58: 1471-1485.

George, J., Janardhan, R., Anand, J. S., Bhagawan, S. S., and Thimas, S. (1996). Melt rheological behaviour of short pineapple fiber reinforced low density polyethylene composites. **Polymer.** 37: 5421-5431.

George, J., Sreekala, M. S., and Thomas, S. (2001). A review on interface modification and characterization of natural fiber reinforced plastic composites. **Polym. Eng. Sci.** 41: 1471-1485.

Herrera-Franco, P. J., and Aguilar-Vega, M. D. J. (1997). Effect of fiber treatment on the mechanical properties of LDPE–henequen cellulosic fiber composites. **J. Appl. Polym. Sci.** 65: 197-207.

Ichazo, M. N., Albano, C., and Gonzalez, J. (2000). Behavior of polyolefins blends with actylated sisal fibers. **Polym. Int.** 9: 1409-1416.

Ichazo, M. N., Albano, C., Gonzalez, J., Perera, R., and Candal, M. V. (2001). Polypropylene/wood flour composites: treatments and properties. **Comp. Struct.** 54: 207-214.

Iannace, S., Ali, R., and Nicolais, L. (2001). Effect of processing conditions on dimensions of sisal fibers in thermoplastic biodegradable composites. **J. Appl. Polym. Sci.** 79: 1084-1091.

Joseph, K., Thomas,S., and Pavithran, C. (1996). Effect of chemical treatment on the tensile properties of short sisal fiber reinforced polyethylene composites. **Polymer.** 37: 5139-5149.

Joseph, K. et al. (1996). Influence of interfacial adhesion on the mechanical properties and fracture behavior of short sisal fiber reinforced polymer composites**. Eur. Polym. J.** 32: 1243-1250.

Joseph, P.V., Joseph, K., and Thomas, S. (1999). Effect of processing variables on the mechanical properties of sisal-fiber-reinforced polypropylene composites. **Comp. Sci. Technol.** 9: 1625-1640.

Joseph, P.V., Joseph, K., Thomas, S., Pillai, C.K.S., Prasad, V.S., Groeninckx, G., and Sarkissova, M. (2003). The thermal properties and crystallisation studied of short sisal fibre reinforced polypropylene composites. **Comp. Part A.** 34: 253-266.

Joseph, P. V., Rabello, M. S., Mattoso, L.H.C., Joseph, K., and Thomas, S. (2002). Environmental effects on the degradation behavior of sisal fibre reinforced polypropylene composites. **Comp. Sci. Technol.** 62: 1357-1372.

Karger-Kocsis, J. (1995). **Polypropylene 1 structure and morphology.** London: Chapman & Hall.

Karnani, R., Krishnan, M., and Naryan, R. (1997). Biofiber-reinforced polypropylene composites. **Polym. Eng. Sci.** 37: 476-483.

Kinloch, A. (1986). **Structural adhesives: Developments in resin and primers**. New York: Elsevier Applied Science.

Krevelen, D. W. (1997). **Properties of polymer.** New York: Elsevier Science.

Liao, B., Hunag, Y., and Cong, G. (1997). Influence of modified wood fibers on the mechanical properties of wood fiber-reinforced polyethylene. **J. Appl. Polym. Sci.** 66: 1561-1568.

Li, Y., Mai, Y., and Ye, L. (2000). Sisal fibre and its composites: a review of recent developments. **Comp. Sci. Technol.** 60: 2037-2055.

Lu, X., Zhang, M. Q., Rong, M. Z., Shi, G., and Yang, G. C. (2003). Self-reinforced melt processable composites of sisal. **Comp. Sci. Technol.** 63: 177-186.

Luo, X., Benson, R. S., Kit, K. M., and Dever, M. (2002). Kudzu fiber reinforced Polypropylene composite. **J. Appl. Polym. Sci.** 85: 1961-1969.

Manchado, M. A. L., Biagiotti, J., Torre, L., and Kenny, J. M. (2000). Effects of reinforcing fibers on the crystallization of polypropylene. **Polym. Eng. Sci**. 40: 2194-2204.

Mieck, K. P., Nechwatal, A., and Knobelsdorf, C. (1995). **Die. Angew. Makromol. Chem.** 225: 37–49. Quoted in Bledzki, A. K. and Gassan, J. (1999). Composites reinforced with cellulose based fibres. **Prog. Polym. Sci.** 24: 221-274.

Mishra, S., Misra, M., Tripathy, S. S., Nayak, S. K., and Mohanty, A. K. (2001). Graft copolymerization of acrylonitrile on chemically modified sisal fibers. **Macromol. Mater. Eng.** 286: 107-113.

Mishra, S., Naik, J. B., and Patil, Y. P. (2000). The compatibilising effect of maleic anhydride on swelling and mechanical properties of plant-fiber-reinforced novalac composites. **Comp. Sci. Technol.** 60: 1729-1735.

Mohanty, A. K., Misra, M., and Hinrichsen, G. (2000). Biofibres, biodegradale polymers and biocomposites: An overview. **Macromol. Mater. Eng.** 276/277: 1- 24.

Mwaikambo, L., Y., and Ansell, M.,P.(1999) .The effect of chemical treatment on the properties of hemp, sisal, jute and kapok for composite reinforcement. **Die. Angew. Makromol. Chem.** 272: 108-116.

Nakorn, W. N., Chinapan. W., and Tepnanraprapai P. (1999). **Factual tips about vetiver grass.** Bangkok: Text and journal.

Plueddemann, E. P. (1982). **Silane coupling agents.** New York: Plenum press.

Quillin, D. T., Yin, M., Koutsky, J. A., and Caulfield, D. F. (1994). Crystallinity in the Polypropylene/Cellulose system. II. crystallization kinetics. **J. Appl. Polym. Sci.** 52: 605-615.

Rana, A. K., Mandal, A., Mitra, B. C., Jacobson, R., Rowell, R., and Banerjee, A. N. (1998). Short jute fiber- reinforced polypropylene composites: effect of compatibilizer. **J. Appl. Polym. Sci.** 69: 329-338.

Ray, D. and Sarkar, B. K. (2001). Characterization of alkali treated jute fibers for physical and mechanical properties. **J. Appl. Polym. Sci.** 80: 1013-1020.

Ray, D., Sakar, B. K., Basak, R. K., and Rana, A. K. (2002). Study of the thermal behavior of alkali treated jute fibers. **J. Appl. Polym. Sci.** 85: 2594-2599.

Razera, I. A. T. and Frollini, E. (2004). Composites based on jute fibers and phenolic matrices: properties of fibers and composites. **J. Appl. Polym. Sci.** 91: 1077-1085.

Rong, M. Z., Zhang, M. Q., Liu, Y., Yang, G. C., and Zeng, H. M. (2001). The effect of fiber treatment on the mechanical properties of unidirectional sisal-reinforced epoxy composites. **Comp. Sċ . Technol.** 61: 1437-1447.

Rowell, R. M. (1989). **International encyclopedia of composites.** 4: 1-16.

Saha, A. K., Das, S., Basak, R. K., Bhatta, D., and Mitra, B. C. (2000). Improvement of functional properties of jute based composite by acrylonitril pretreatment**. J. Appl. Polym. Sci.** 78: 495-506.

Saheb, D. N. and Jog, J. P. (1999). Natural fiber polymer composites: A review. **Adv. Polym. Technol.** 18: 351-363.

Sanadi, A.R., Caulfield, D. F., Jacobson, R. E., and Rowell, R. M. (1995). Renewable agricultural fibers as reinforcing fillers in plastics: mechanical properties of kenaf fiber polypropylene composites. **Amer. Chem. Socie.** 34: 1889-1896.

Schuh, T. G. (1999). Renewable Materials for Automotive Applications.

Singh, B., Gupta, M., Verma, A., and Tyagi, O. (2000). FT-IR microscopic studies on coupling agents: treated natural fibres. **Polym. Int.** 49: 1444-1451.

Sydenstricker, T. H. D., Mochnz, S., and Amico, S. C. (2003). Pull-out and other evaluations in sisal-reinforced polyester biocomposites. **Polym. Test**. 22: 375-380.

Valadez-Gonzalez, A., Cervantes-Uc, J. M., Olayo, R., and Herrera-Franco, P.J. (1999). Effect of fiber surface treatment on the fiber matrix bond strength of natural fiber reinforced composites. **Comp: Part B.** 30: 309-320.

Valadez-Gonzalez, A., Cervantes-Uc, J. M., Olayo, R., and Herrera-Franco, P.J. (1999). Chemical modification of henequen fibers with an organosilane coupling agent. **Comp: Part B.** 30: 321-331.

Van Der Oever, M. J., Bos, H. L., and Kemenade, M. (2000). Influence of the physical structure of flax fibres on the mechanical properties of flax fibre reinforced polypropylene composites. **Appl. Comp. Mater.** 7: 387-402.

Varma, I. K., Krishnan, S. R.A., and Krishnamoorthy, S. (1987). Effect of chemical treatment on thermal behavior of jute fibers. **Text. Res. J.** 486-494.

Wambua, P., Iens, J., and Verpoest, I. (2003). Natural fibres: can they replace glass in fibre reinforced plastics. **Comp. Sci. Technol.** 63: 1259-1264.

Wang, Y., Na, B., Fu, Q., and Men Y. (2004). Shear induced shish-kebab structure in PP and its blends with LLDPE. **Polymer.** 45: 207-215.

Wielage, B., Lampke, T., Marx, G., Nestler, K., and Starke D. (1999). Thermogravimetric and differential scanning calorimetric analysis of natural fibres and polypropylene. **Thermo. Acta.** 337:169-177.

Zafeiropoulos, N. E., Baillie, C.A., and Matthews, F. L. (2001). A study of transcrystallinity and its effect on the interface in flax fibre reinforced composite materials. **Comp. Part A.** 32: 525-543.

APPENDIX A

CHEMICAL STRUCTURES OF CELLULOSE

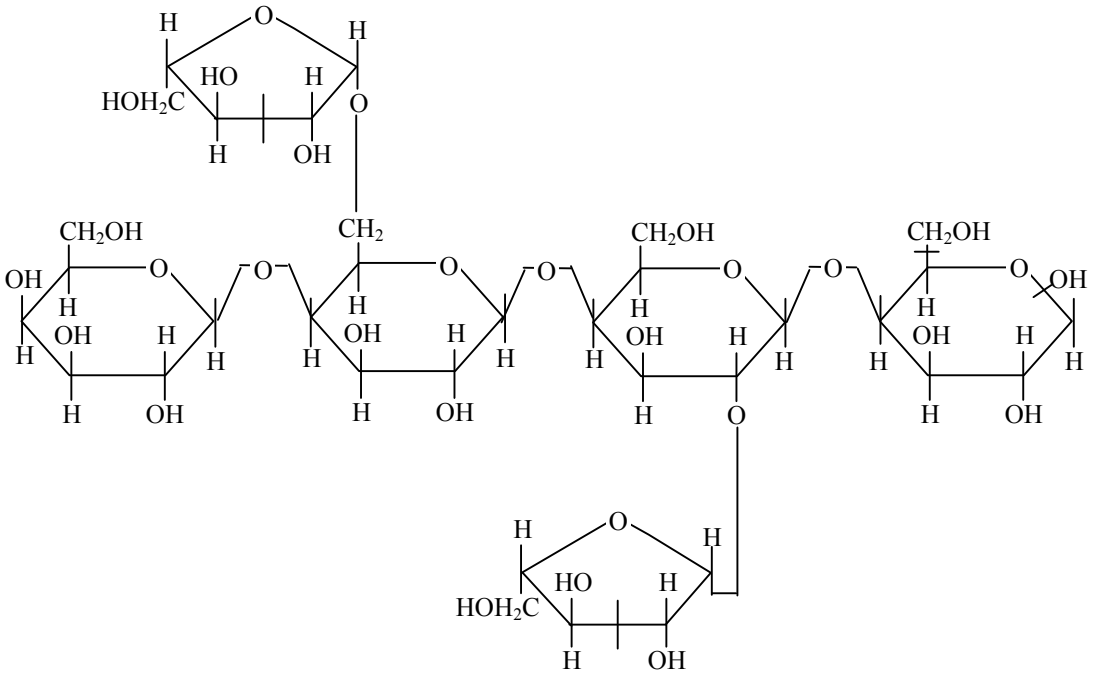

(a)

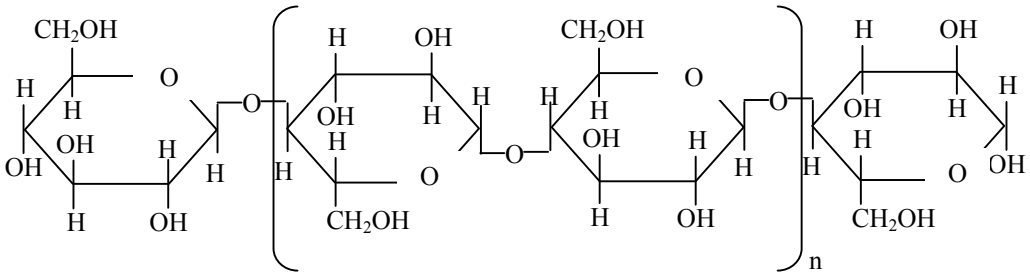

(b)

Figure A.1 Chemical structures of (a) hemicellulose and (b) cellulose

APPENDIX B

RESULTS OF CHEMICAL COMPOSITIONS OF VETIVER GRASS

Table B1 Chemical compositions of VL, NaOH-VL, and VF.

Chemical compositions	**VL**	**NaOH-VL**	**VF**
C	89.39 wt%	97.30 wt%	99.00 wt%
Na_2O	0.00 wt%	0.01 wt%	0.00 wt%
MgO	0.07 wt%	0.07 wt%	0.07 wt%
Al_2O_3	0.14 wt%	0.05 wt%	0.02 wt%
SiO_2	5.74 wt%	1.17 wt%	0.34 wt%
P_2O_5	0.33 wt%	0.12 wt%	0.03 wt%
SO_3	0.28 wt%	0.05 wt%	0.02 wt%
Cl	0.07 wt%	0.02 wt%	0.01 wt%
K_2O	3.34 wt%	0.21 wt%	0.02 wt%
CaO	0.49 wt%	0.89 wt%	0.46 wt%
Sc	0.75 ppm	14.99 ppm	12.42 ppm
TiO_2	28.79 ppm	16.09 ppm	0.00 wt%
V	0.00 wt%	0.00 wt%	0.62 ppm
Cr	25.66 ppm	11.25 ppm	1.32 ppm
MnO	0.05 wt%	0.04 wt%	0.02 wt%
Fe_2O_3	0.06 wt%	0.04 wt%	40.53 ppm
Co	3.30 ppm	0.00 wt%	0.91 ppm
Ni	24.80 ppm	7.84 ppm	2.25 ppm
Cu	61.00 ppm	29.25 ppm	18.52 ppm
Zn	45.68 ppm	62.85 ppm	39.45 ppm
Ga	1.31 ppm	0.08 ppm	0.40 ppm

Table B1 Chemical compositions of VL, NaOH-VL, and VF (continued)

Chemical compositions	VL	NaOH-VL	VF
Ge	0.00 wt%	0.09 ppm	0.01 ppm
As	0.00 wt%	0.00 wt%	0.00 wt%
Se	0.22 ppm	1.10 ppm	0.49 ppm
Br	84.89 ppm	7.73 ppm	1.49 ppm
Rb	21.45 ppm	1.63 ppm	0.93 ppm
Sr	21.05 ppm	34.69 ppm	14.04 ppm
Y	1.15 ppm	1.91 ppm	0.00 wt%
Zr	5.73 ppm	2.38 ppm	0.00 wt%
Hf	15.48 ppm	6.40 ppm	0.81 ppm
Ta	0.00 wt%	5.97 ppm	4.62 ppm
W	0.00 wt%	0.00 wt%	0.00 wt%
Hg	12.46 ppm	6.01 ppm	0.00 wt%
Tl	0.00 wt%	2.52 ppm	0.00 wt%
Pb	0.00 wt%	1.44 ppm	4.97 ppm
Bi	0.00 wt%	5.36 ppm	5.63 ppm
Th	0.00 wt%	0.00 wt%	1.28 ppm
U	0.00 wt%	2.88 ppm	1.57 ppm
Nb	0.00 wt%	0.34 ppm	0.00 ppm
Mo	1.25 ppm	0.74 ppm	0.00 wt%
Ag	1.07 ppm	0.66 ppm	0.35 ppm
Cd	0.18 ppm	0.00 wt%	0.00 wt%

Table B1 Chemical compositions of VL, NaOH-VL, and VF (continued)

Chemical compositions	VL	NaOH-VL	VF
In	1.55 ppm	0.17 ppm	0.29 ppm
Sn	1.61 ppm	1.18 ppm	0.49 ppm
Sb	0.77 ppm	0.14 ppm	0.00 wt%
Te	0.00 wt%	0.52 ppm	0.41 ppm
In	4.89 ppm	0.00 wt%	0.48 ppm
Cs	0.00 wt%	0.25 ppm	0.84 ppm
Ba	13.22 ppm	6.99 ppm	3.49 ppm
La	0.00 wt%	0.00 wt%	0.00 wt%
Ce	0.00 wt%	2.48 ppm	0.00 wt%
Pr	0.00 wt%	0.00 wt%	0.00 wt%
Nd	0.00 wt%	0.00 wt%	0.00 wt%

APPENDIX C

RESULTS OF MECHANICAL PROPERTIES OF VETIVER-PP COMPOSITES

Equation for calculating tensile strength, Young modulus and elongation at break of vetiver-PP composites

$$\text{Tensile strength} = \frac{\text{Load (N)}}{\text{Cross section area } (\text{mm}^2)}$$

$$\text{Young' s modulus} = \frac{\text{Stress } (\text{MPa})}{\text{Strain } \left(\frac{\text{mm}}{\text{mm}}\right)}$$

$$\text{\% Elongation at break} = \frac{\text{Ultimate length} - \text{Original length } (\text{mm})}{\text{Original length } (\text{mm})} \times 100\ \%$$

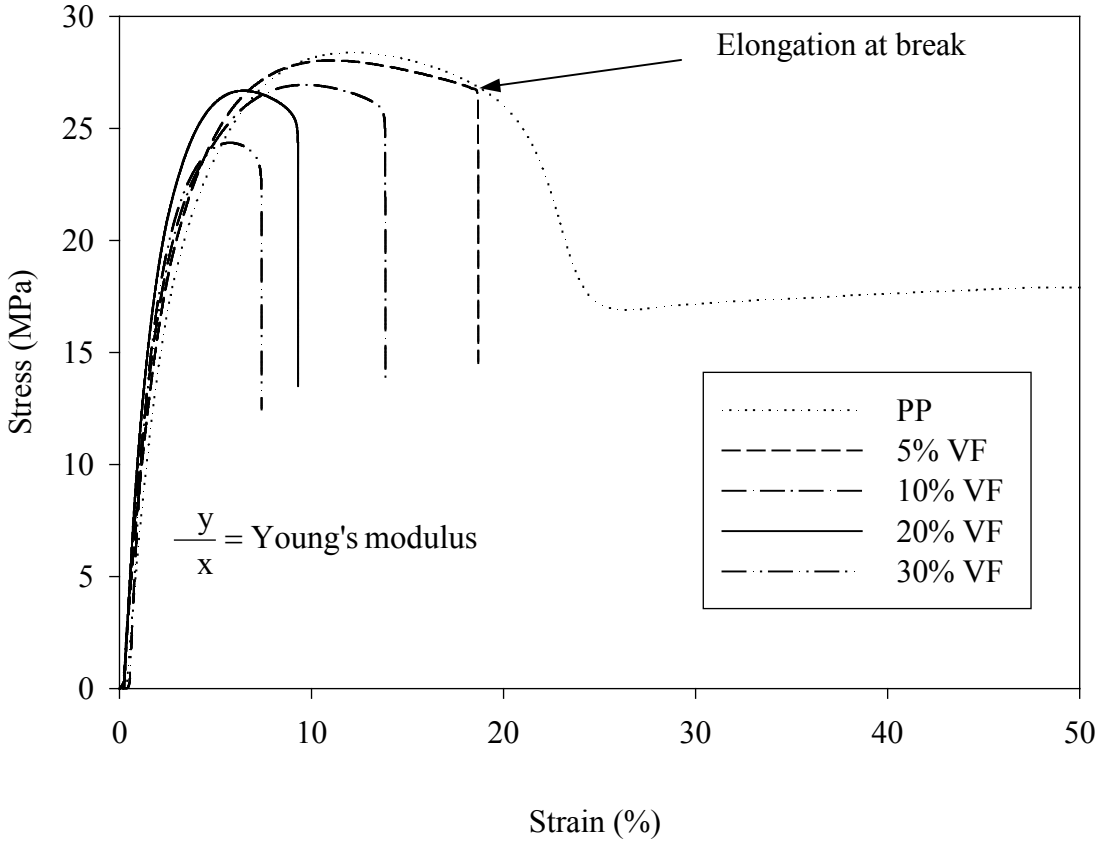

Figure C.1 Stress-strain curves of vetiver-PP composites from VF at various vetiver contents.

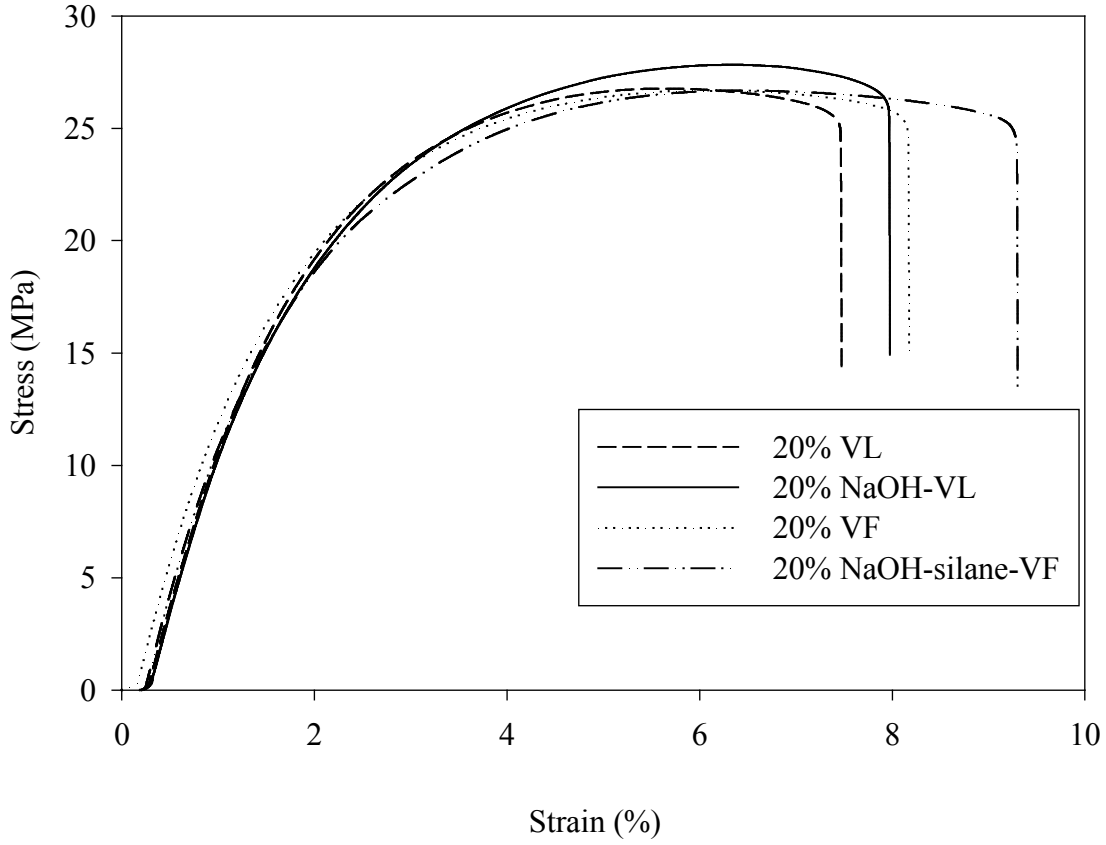

Figure C.2 Stress-strain curves of vetiver-PP composites from VL, NaOH-VL, VF, and NaOH-silane-VF at 20% vetiver content.

BIOGRAPHY

Miss Wandee Thuamthong was born on May 11, 1979 in Rayong, Thailand. She earned her Bachelor's Degree in Polymer Engineering from Suranaree University of Technology (SUT) in 2001. She then continued her Master's degree in Polymer Engineering at School of Polymer Engineering, Institute of Engineering at Suranaree University of Technology. Her expertise is in the field of polymer processing and polymer composites. During her Master's degree study, she presented two papers. One entitled "Thermal, Rheological, Mechanical, and Morphological Properties of Vetiver-Polypropylene Composites" in the 8th Pacific Polymer Conference (PPC8), Bangkok, Thailand. Another entitled "Effect of Vetiver Contents and Vetiver Lengths on Mechanical and Morphological Properties of Vetiver-Polypropylene Composites" in the third Thailand Materials Science and Technology Conference, Bangkok, Thailand.